DEVELOPMENT AND MECHANICAL PERFORMANCE OF SUSTAINABLE GEOPOLYMER CONCRETE

by

Ghina M. Zannerni

A Thesis Presented to the Faculty of the
American University of Sharjah
College of Engineering
In Partial Fulfillment
Of the Requirements
For the Degree of

Master of Science in
Civil Engineering

Sharjah, United Arab Emirates

May 2016

Approval Signatures

We, the undersigned, approve the Master‘s Thesis of Ghina M. Zannerni.

Thesis Title: Development and Mechanical Performance of Sustainable Geopolymer Concrete

Signature	**Date of Signature** (dd/mm/yyyy)
_____	_____
Dr. Adil Tamimi Professor, Department of Civil Engineering Thesis Advisor	
_____	_____
Dr. Kazi Fattah Assistant Professor, Department of Civil Engineering Thesis Co-Advisor	
_____	_____
Dr. Mohammad AlHamaydeh Associate Professor, Department of Civil Engineering Thesis Committee Member	
_____	_____
Dr. Tarik Ozkul Professor, Department of Computer Science and Engineering Thesis Committee Member	
_____	_____
Dr. Aliosman Akan Head, Department of Civil Engineering	
_____	_____
Dr. Mohamed Guma El-Tarhuni Associate Dean, College of Engineering	
_____	_____
Dr. Leland Blank Dean, College of Engineering	
_____	_____
Dr. Khaled Assaleh Interim Vice Provost for Research and Graduate Studies	

Acknowledgment

I would like to thank first my thesis advisor Dr. Adil Tamimi from the college of engineering at the American University of Sharjah (AUS). The door to Dr. Tamimi‘s office was always open to me whenever I needed his knowledge to solve a problem I faced during the laboratory work or my research writing. His telephone was also ready to answer my calls whenever I had a question or faced a trouble during my thesis work. He consistently pushed me to work hard, which I really needed to make the work be my own and done on time.

I would also like to acknowledge Dr. Kazi Fattah, my co-advisor of this thesis, for his valuable comments and information in his knowledge area, and as the second reader of this thesis who continuously gave me advice and comments to improve my work.

My thanks also go to the experts who were involved in the completion and validation of the laboratory work of this thesis for their support and help: Mr. Thomas Job from the Chemistry Department at AUS, Mrs. Fathia Mohammed from the Department of Chemical Engineering at AUS and Mr. Mohammed Ansari from the Department of Civil Engineering.

Furthermore, I am very grateful for my colleague Eng. Abdullah M. Sagher for his continuous help especially through the heavy lab work that needed man‘s muscles, a task that I could not have achieved alone. I owe him deep respect and gratefulness.

Most importantly, my deep and sincere thanks go always to my parents and siblings who supported me the most in my hard times, helped me with their love and patience to overcome a crisis I faced, and continuously help me to reach my goals towards prosperity.

Finally, I appreciate the GTA support I received from the Department of Civil Engineering at AUS during my graduate study. Special thanks go to Dr. Aliosman Akan, the head of the Department of Civil Engineering.

Abstract

Concrete production has always been a main source of carbon dioxide (CO_2) emissions. These emissions come mainly from Ordinary Portland Cement (OPC), which releases an average of 0.83 tons of CO_2 /t. Researchers have been trying to find a suitable substitute for the OPC as a binding material in concrete to meet sustainability requirements. Therefore, this study focuses on developing and evaluating sustainable geopolymer concrete. Three cementitious materials, Class F fly ash, ground granulated blast furnace slag (GGBS), and silica fume, were used with different combinations to replace all cement in the mix. A 10 M sodium hydroxide solution was prepared and used to activate the cementitious materials and form geopolymer paste. Seven different concrete mixes were developed and analyzed in terms of strength, durability, microstructural performance, and carbon footprint with the aim of choosing the geopolymer concrete mix with the best performance. A total of 102 concrete samples, including cubes, beams, and cylinders were casted and tested for compressive strength, tensile strength, flexural strength, and modulus of elasticity. A durability test was performed on the geopolymer concrete specimens using rapid chloride penetration test. A microstructural analysis was also performed on the specimens using scanning electron microscope (SEM) coupled with energy dispersive X-ray spectra (EDS) to evaluate the geopolymer concrete microstructure. The experimental results of geopolymer concrete were compared with a control mix that had 100% OPC. Results showed good performance of geopolymer concrete with 100% replacement of cement by GGBS in compressive strength, flexural strength, tensile strength, and chloride penetration tests. It showed a compressive strength of 36 MPa at 28 days without the need for heat curing, and a tensile strength that was higher than the control mix by 12%. SEM images showed high compactness and no cracks in the ambient cured specimens of the mix with 100% GGBS, and the EDS images showed high traces of both alumino-silicate and calcium silicate gels responsible for strength gain in geopolymer concrete. Furthermore, analysis of the concrete mixes showed that the use of geopolymer concrete has the potential to decrease the carbon footprint of concrete production for up to 60%.

Search terms: *Geopolymer concrete, sustainability, carbon footprint, green concrete, SEM analysis, mechanical performance, RCPT.*

Table of Contents

List of Tables

List of Figures

Chapter 1: Introduction to Geopolymer Concrete

1.1 Background

1.1.1 Carbon footprint of the current concrete production. With the increase in global population and need for more infrastructures, the production and use of concrete has reached enormous proportions. Concrete production has always been a main source of carbon dioxide (CO_2) emissions. There is approximately 3 billion tons of cement produced globally each year. This contributes to 8% of the global production of CO_2 emissions [1], [2]. The carbon footprint resulted from the production of Ordinary Portland Cement (OPC), which is the main binding agent in concrete, can be measured as 1000 kg of carbon/m^3 [3], [4]. The breakdown of the sources of CO_2 emissions in concrete production can be as follows [5]:

- Emissions related to coarse aggregate

These emissions are due to excavators that work with diesel power, and haulers that move the aggregate from quarries to crushing equipment and then into stockpiles. Moreover, the electricity used in the crushing and screening machines is a main source of CO_2 emissions in coarse aggregate production.

- Emissions related to fine aggregate

These emissions are due to diesel in excavators used in strip-mining process, and haulers that move the sand from mining process to grading equipment, and due to electricity used in grading machines.

- Emissions related to cement or cementitious materials such as fly ash and GGBS

These are due to cement manufacture by decomposing limestone at the kiln at a very high temperature. Every ton of CaO (coming from the chemical composition of cement or/and cementitious material) produces 0.5 ton of CO_2 emissions. A very little portion of the CO_2 emissions will be then absorbed by the concrete through its lifetime in a process called carbonation illustrated in equation (1). This small portion will not be accounted for in the carbon emissions calculations.

$$Ca(OH)_2 + CO_2 \rightarrow CaCO_3 + H_2O \quad (1)$$

CO_2 emissions associated with fly ash and GGBS are due to the initial production of coal and steel, collecting and milling process, refining process, and transporting.

- Emissions related to admixtures

This contributes to a very small portion of concrete CO_2 emissions. Therefore, it will not be considered in the calculations in this study.

- Emissions related to concrete mixing, transporting, and placing

These emissions are due to electricity consumed in mixer, and diesel fuel consumed for transportation, vibration, pumping, and finishing.

Figures 1-3 show the breakdown of CO_2 emissions for different concrete production activities.

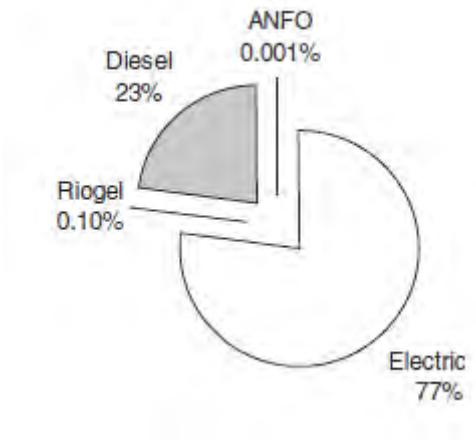

Figure 1: CO_2 emissions breakdown for basalt coarse aggregate [5]
ANFO: Ammonium Nitrate Fuel Oil.

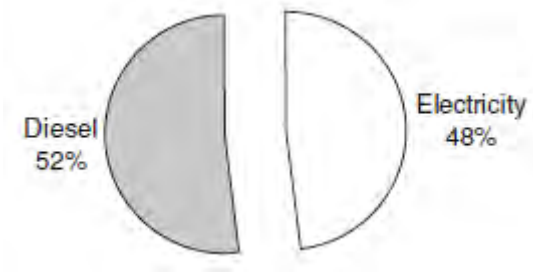

Figure 2: CO_2 emissions breakdown for fine aggregate [5].

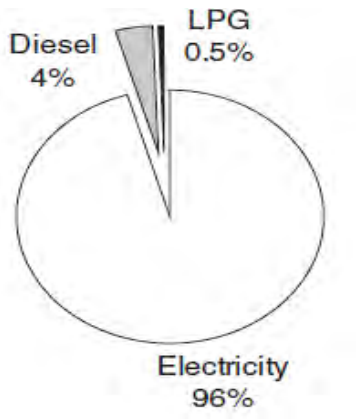

Figure 3: CO_2 emissions breakdown for concrete batching, LPG: Liquid Petroleum Gas [5].

OPC does not only release harmful greenhouse gases (GHGs) such as CO_2, but also releases a large amount of dust during manufacturing, and it is energy intensive. For these reasons, a need for a more sustainable binding material has increased [6]. Since cement is the main contributor in concrete production that has a high negative impact on the environment, several solutions world-wide have been recommended, tested, and adopted in the field of concrete production in order to reduce or eliminate this environmental impact. Such concrete is so called —green" to indicate that it is being produced in an environmentally friendly way [4], [7].

The word —green" is usually given for the concrete that has low CO_2 emissions. This concrete can be obtained by various ways such as partial replacement of cement by other supplementary materials like slag or fly ash. Several studies are being carried out to find a more environmentally friendly method of concrete preparation. Heede and Belie [8] reported that a 25% reduction of CO_2 emissions can be achieved by replacing only 10% of cement by any type of cement supplementary materials [8]. The use of cement supplementary materials such as GGBS does not only reduce the carbon footprint, but also reduces the heat generation in concrete, reduces the water and salt permeability, and improves the service life of the structure [3]. Another way to reduce the CO_2 emissions of concrete is to increase its compressive strength by decreasing the water to cement ratio. By doing so, smaller dimensions of the structural elements will be required; therefore, less amount of cement will be used which will reduce CO_2 emissions. In general, increasing the

desired compressive strength of concrete by the double reduces CO_2 emissions by 30% [8].

1.1.2 Geopolymer as a green concrete. Researchers are recently trying to find more suitable substitutes to the OPC as a binding material in concrete production due to sustainability requirements. Zhang et al. [1] reviewed the use of geopolymer binders as an alternative to OPC in concrete production. Geopolymer binder is produced by the activation of silica and solid alumina in high alkalinity producing materials. Geopolymer concrete is a new material that is still under research and has limited applications. According to Zhang et al. [1], geopolymer has been proposed as a good binder to replace cement in concrete in order to reduce carbon footprint and save energy, but at the same time not sacrificing performance. It will be a leading material in the future of renewable resources and waste control as mentioned by Motorwala [9].

Geopolymer binders as a term was given to alkali activated alumino-silicate materials by Joseph Davidovits in the 1970s. These materials were first used for fire protection before being used in more structural applications such as replacing the OPC. Geopolymers are believed to have a good resistance to fire due to its ceramic-like behavior at high temperatures [10]. It also has good resistance to thermal shrinkage [10]. However, it was reported that porosity is the main microstructural property that limits the mechanical behavior of geopolymer concrete [11]. Unlike normal concrete, matrix formation and strength development of geopolymer concrete does not need the calcium silicate hydrate (C-S-H) gel to be formed. However, it gains its strength from the alumino-silicate polycondensation [7]. The chemical composition of geopolymers consists of tetrahedral silicate and aluminate ions arranged in a three dimensional structure with covalent bonds (see Figure 4). The tetrahedral Al (III) ion has negative charges associated with it, which the alkali cations will balance. Geopolymer binders do not need the presence of cement. To produce such binder, two raw materials are needed: reactive solid that is alumino-silicate material such as calcinated clay or fly ash (to provide Si and Al), and an activating solution that is alkaline in nature such as silicate solution or hydroxide solution (to provide the positive ion). A slightly high temperature is needed in most cases to initiate the reaction of geopolymerization [12], [2]. Nowadays, studies are

being carried out to produce geopolymer binders from one raw material instead of two; however, a strength that is enough for construction applications has not yet been achievable. The reaction moves through the following steps: first, the dissolution of Si and Al in the alkaline solution to form monomers where the activating solution dissolves the soluble phase of the source material such as fly ash and releases alumina and silica out from the surface of the particles of fly ash. Second, the transportation of these monomers takes place to form the initial gel where the silicate and aluminate react with the alkalis in the activating solution to form the alumino-silicate gel around the fly ash particles. Finally, these species condensate and harden [6]. Through the mixing procedure, geopolymer paste (the reactive solid along with the activating solution) can be mixed with any type of coarse and fine aggregate used with the OPC [12]. In the chemical reaction that forms the geopolymer concrete, the silicate and aluminate in the supplementary material such as fly ash react with the alkaline solution such as sodium hydroxide (NaOH) and sodium silicate (Na_2SiO_3) to form a gel that acts like a binder for the coarse and fine aggregates. This resulting gel has a ring structure that consists of three dimensional polymeric chain. The main bonds in it are the Si-O-Al-O bonds. (See Figure 4.)

The equations that describe the formation of geopolymer concrete out of its base materials are shown in Figure 4 as a sequence from A to B.

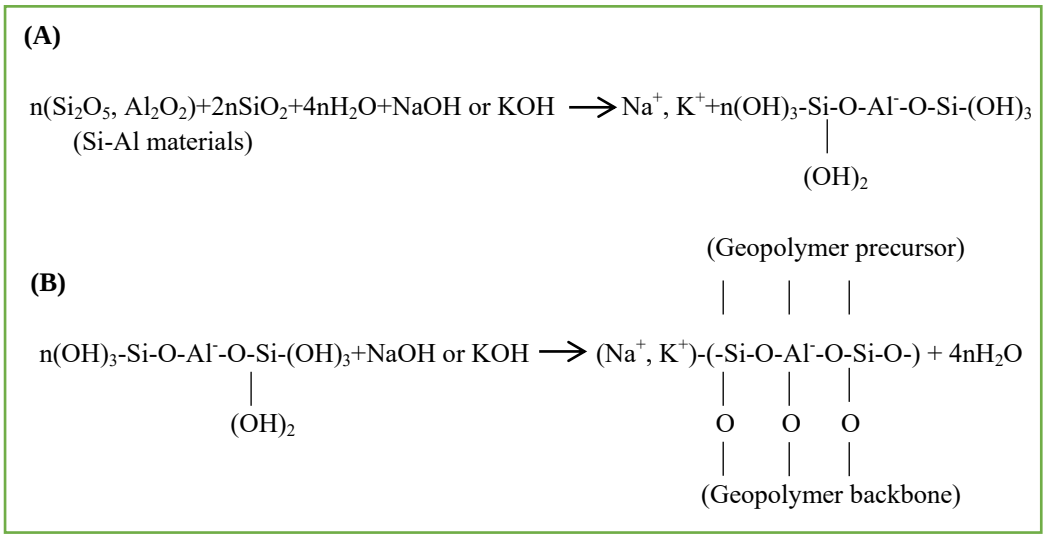

Figure 4: Formation of geopolymer concrete [13].

1.1.3 Geopolymerization reaction. As a result of the geopolymerization reaction shown in Figure 4, water will be produced with the geopolymers in the

concrete and both appear at the end of the chemical geopolymerization equation. This water will be spelled out during drying or curing stage, leaving behind very small pores that are beneficial for the concrete performance. Hence, water added to the geopolymer concrete matrix will play no role in the reaction of geopolymerization. It only enhances the workability of the concrete during mixing and handling. In contrast, water plays the most important role for cement hydration reaction in normal concrete [9].

The reaction of geopolymerization is considered a fast chemical reaction in the presence of Si-Al material with alkaline. The resultant geopolymer is an inorganic polymer that has an amorphous microstructure, and chemical bonds of Si-O and Al-O. If the source material contains Ca ions, this will increase the strength of geopolymer concrete. Ca^{+2} ions (along with Na^{+}) will compensate the Al^{+3} ions when fly ash dissolves by the alkaline solution. When the microstructure of geopolymer concrete is tested, crystalline hydrates cannot be detected. In general, geopolymer binder has the following chemical formula: Mn [-(Si-O)z –Al-O]n. w(H_2O), where M is the cation from the alkaline solution such as sodium or potassium, n is the degree of geopolymerization, and z is a real number from 1 to 32 [1].

In terms of sustainability, geopolymer concrete is mainly made of waste materials such as fly ash, silica fume, or GGBS. If the use of geopolymer concrete is implemented, cement will no longer be needed in the concrete mix. Consequently, concrete preparation will produce lower CO_2 emission. Moreover, using fly ash or calcinated clay as raw materials in the geopolymer is not as energy intensive or produces as high CO_2 emissions as OPC does. However, the production of the activating alkali solution such as sodium silicate or sodium hydroxide is relatively energy intensive (for sodium silicate, energy consumption is 5.4 GJ/t, and for dry sodium hydroxide, it is 14.9 GJ/t, while for OPC, it is 3.2 GJ/t) [1]. Although the production of the activating solution is energy intensive, it does not represent more than 10% of the weight of the materials in the mix design. Moreover, CO_2 emissions resulting from the production of geopolymer binder are 80% less than the emissions of OPC [1], which will help in the overall reduction of CO_2 in a "green" concrete.

1.1.4 Fly ash effect. Fly ash is a by-product of the combustion of coal that is transported from the combustion zone to particle collecting zone using fuel gasses. Its particles are finer than cement and spherical in shape. The size of fly ash particles ranges from 1 to 150 micrometers. Chemically, it mainly contains silicon oxide (SiO_2), aluminum oxide (Al_2O_3), calcium oxide (CaO), and iron oxide (Fe_2O_3). It also contains some elements in smaller amounts such as sulphur, magnesium, titanium, sodium, and potassium. In normal concrete, fly ash is used in industry as a replacement of cement up to 60% [9]. Calcium hydroxide that results from the hydration of cement reacts with the silicon oxide in the fly ash particles to form a gel of calcium silicate hydrate (C-S-H). The use of fly ash in normal concrete improves its workability and reduces the water content due to the spherical shape of its particles. Moreover, it improves concrete density and durability due to the small particle size that acts as filler [9], [14]. It also enhances the confinement of the geopolymer concrete by increasing the particle packing and reducing its porosity.

The properties of fly ash vary widely based on the chemical composition and the impurities of the source coal prior to combustion, and the properties of the combustion process [14]. Two main types of fly ash are present: Class (F), and Class (C). The most commonly used type of fly ash in the production of geopolymer concrete is class (F), and it is more analyzed in literature than class (C) due to its large availability, sufficient silica and alumina content, and low water demand [15]. However, class C fly ash contains more Ca than class F [14]. Generally, fly ash has less amount of Ca than GGBS. Precursor materials with high amount of CaO were reported to give higher strength geopolymer concrete. It was also reported that it reduces the sitting time of concrete. Moreover, it was found to improve the mechanical properties of the geopolymer samples cured at ambient temperature. This was justified by the formation of calcium silicate hydrate (C-S-H) in the material containing high amount of CaO along with the alumino-silicate hydrate of the geopolymer reaction [15].

1.1.5 GGBS effect. GGBS is a by-product of iron manufacturing that has calcium alumino-silicate microstructure. GGBS has a chemical structure that contains sufficient calcium for charge-balancing the aluminum. It was found that GGBS particles reaction depends on the size of the particles. Particles greater than 2

micrometers react slowly, while particles less than 2 microns in size react faster and need 24 hrs to be reacted completely in both normal and geopolymer concretes [14]. Addition of GGBS to fly ash based geopolymer concrete was found to have a positive impact on the strength of concrete even when added in small amounts as 4%. However, the impact depends on the type and concentration of the activating solution, and the percentages of GGBS and fly ash relative to each other [15].

1.1.6 Silica fume effect. Silica fume is one of the pozzolanic materials that are often mixed with cement as replacement. It is sometimes referred to as micro-silica, and it is a by-product of silicon alloys. Silica fume is a very fine material that has a large amount of silicon dioxide which enhances its pozzolanic effect. It enhances the microstructure, the mechanical properties, and durability of normal concrete [16]. The use of silica fume as well as other cementitious materials also has economic and environmental advantages in concrete in general. In particular, tests show that silica fume reduces the normal concrete permeability towards water and chloride. In addition, it increases the late strength of concrete due to the reaction between the pozzolanic material and CH that is released after the hydration of C_2S and C_3S. In the concrete mix, silica fume was found to act mostly in the transition zone between the aggregate and the cement paste due to the fact that this zone has higher porosity and CH concentration than in the cement paste. Experimental investigation by Abd Elaty and Ghazy [17] used Portland cement with four different percentages of silica fume, 0, 10, 20, and 30%. The results showed that increasing the percentage of silica fume resulted in higher compressive strength of concrete up to 20% replacement, where beyond this percentage the strength started to decrease. This indicates that there is an optimum percentage of silica fume to be introduced to the concrete mix [17]. According to Abd Elaty and Ghazy [17], at the fresh stage, silica fume causes delay in the initial and the final setting times and reduces the slump. For that reason, it is preferable to use superplasticizer whenever silica fume is used. It also delays the strength gain; however, it increases the final strength of concrete. According to Khedr and Abou-Zeid [16], the increase in the silica fume content results in lower slump, which is related to its large surface area. In addition, the reason behind the delay of strength gain is the pozzolanic effect on strength, which takes time to happen. Khedr and Abou-Zeid [16] also state that the introduction of

silica fume in the concrete mix improves its flexural strength due to its ability to fill the voids. This fact applies up to 20% replacement; however, beyond this percentage, there will be no more improvement in the flexural strength of concrete. The same also applies to the modulus of elasticity of concrete. Silica fume also enhances the bond between steel reinforcement and concrete and reduces the pullout. This is due to the reduction of the amount of water at the zone between the steel and concrete [16].

In the case of geopolymer concrete, the same effect illustrated above was reported by [7], [18], [19], & [20] about using silica fume in geopolymer concrete mix. More detailed effects of silica fume on geopolymer concrete are discussed in proceeding sections.

1.1.7 Aluminum effect. It was found that the amount of aluminum available in the source material, and the rate it is being released at, control over the strength of the geopolymer concrete, its microstructure, setting, and acid resistance. The release of aluminum from the source material depends on the concentration and type of the alkali activator. Silicon availability also affects the geopolymer concrete properties but to a lesser extent [12].

1.1.8 Alkalis effect. Researchers have found that the best alkaline solution to be used in geopolymer concrete is a combination of silicate and hydroxide of either sodium or potassium. However, the use of one alkaline solution like sodium hydroxide (NaOH) is also feasible. It was found that the type of alkaline solution used in the gepolymer concrete affects the geopolymarization process. For example, NaOH was reported to have higher rate of geopolymerization reaction than potassium hydroxide (KOH). NaOH dissolves the minerals in the source material at a higher rate than KOH [9].

The amount of alkaline solution used in the geopolymer mix affects the properties of the fresh and hardened concrete as reported by [6]. Different amounts of alkaline solution, 35%, 40%, and 45% (by volume of the mix) were tested. The higher percentage of the liquid alkaline is used, the higher are the slump and the sitting time obtained. However, increasing the amount of alkaline solution leads to less compressive strength as found by [6]. Moreover, the ratio of the two alkali solutions

relative to each other has a varying effect on the workability and strength as well. For example, Ravikumar et al. [6] reported lower workability and sitting time when the ratio of sodium silicate to sodium hydroxide was increased from 1.5 to 2.5.

1.1.9 SEM and EDS. Scanning electron microscopy (SEM) is used to study the internal structure and morphology of specimens; whereas, energy dispersive X-ray spectra (EDS) is used to identify the chemical composition of the specimens. Ravikumar et al. [6] found that the SEM images of geopolymer concrete specimens show more unreacted particles of fly ash when lower concentration of NaOH is used as shown in Figure 5. The geopolymer reaction forms an alumino-silicate gel that covers the fly ash particle. This gel is a result of the dissolving of silica and alumina from the fly ash particle and their reaction with the alkali solution to then condense on the surface of fly ash. The geopolymer reaction becomes of a slow rate when the fly ash particle is completely covered by the alumino-silicate gel. Ravikumar et al. [6] indicate that reacted particles can be distinguished by having higher levels of Na, and lower level of Si and Al than the unreacted ones.

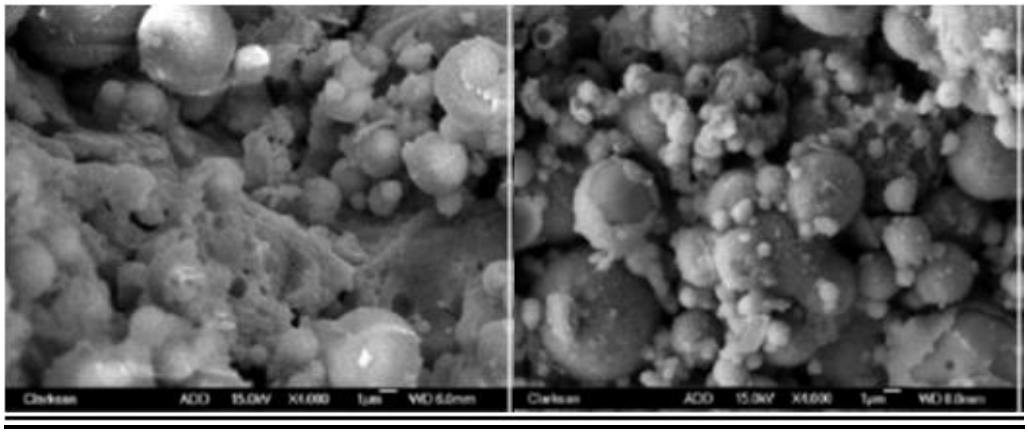

Figure 5: 8 M (on the right) has more reacted particles than 4 M (on the left) [6].

In the case of GGBS, particles cannot be identified individually as in the case of fly ash. In fact, GGBS binder is more homogeneous and compact. Higher concentration of NaOH leads to a less porous material of GGBS-based binder. The reaction product in the case of GGBS has higher amount of Ca and lower amount of Al than in the case of fly ash. It is mainly calcium silicate hydrate gel (C-S-H) reacted areas in the case of GGBS that can be identified by a more crystalized form than the

unreacted areas as shown in Figure 6. It can also be said that the reaction product in the case of GGBS is more amorphous than the reaction product of fly ash [6].

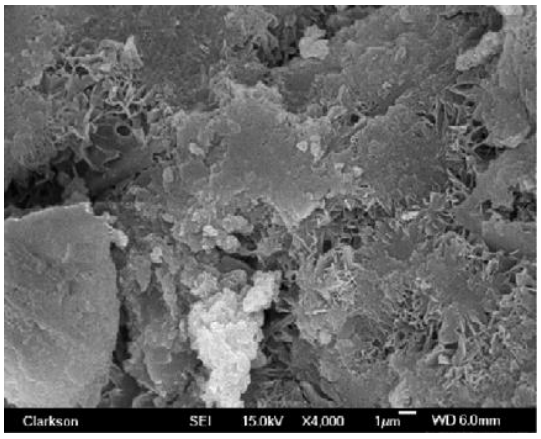

Figure 6: Crystalized areas refer to reaction product of GGBS-based binder [6].

1.2 Research Objectives

This research develops and assesses the mechanical performance of geopolymer concrete specimens of the best performance mix selected. It aims at the following:

- Developing geopolymer concrete mixes using zero cement and cured at ambient temperature.
- Evaluating the mechanical behavior of the geopolymer concrete specimens.
- Analyzing the microstructural properties of the geopolymer concrete specimens.
- Evaluating the durability of the geopolymer concrete specimens.
- Evaluating the carbon footprint of the geopolymer concrete.

1.3 Literature Review

As the demand for a more sustainable binding material in concrete other than cement is increasing, more detailed research on this topic is required. The area of geopolymer –as a new green and environment friendly material- is being explored by researchers and engineers all over the world. Fresh and hardened stage properties, durability, and microstructure of geopolymer concretes are now of a huge concern.

After surveying the literature, a number of the several investigations that focused on geopolymer concrete are reported in this section.

1.3.1 Mechanical properties of geopolymer concrete. Diaz-Loya and Allouche [12] tested the effects of using fly ash from different sources on the mechanical properties of the geopolymer concrete (GPC). They based their study on the fact that fly ash that has optimum properties will lead to the best geopolymer concrete in terms of mechanical behavior- if the design of the mixes and the curing conditions were fixed-. They were able to develop an empirical model that finds the mechanical behavior of the GPC, knowing the characteristics of the fly ash used. The activating solution used was sodium silicate and14 M NaOH solution. The researchers mixed the two solutions in a ratio of 1:1 by weight. The fine aggregate used in the mix was well-graded sand, and the coarse aggregate was Pea gravel. High range superplasticizer was added to the mix at the last 60 seconds of mixing in order to get a slump of 10-15 cm. The mixing procedure went through the following steps:

1- Mixing fly ash with the solution of NaOH for 30 seconds.
2- Adding Sodium Silicate and mixing for 30 seconds.
3- Adding coarse aggregate and mixing for 120 seconds (in the last 60 seconds, the superplasticizer was added).

Cylindrical molds were used for the compressive strength according to ASTM C39, and other cylindrical specimens were used for the Elastic Modulus test according to ASTM C469. Moreover, flexural strength was tested using a third point load according to ASTM C78. The experimental results showed that 95% of f'_c (compressive strength) and f_r (flexural strength) were reached through the first 3-5 days. Geopolymer concrete density was also measured in the study, and it varied between 1890-2371 kg/m^3. The results of the flexural strength were between 2.24-6.41 MPa. Modulus of elasticity values ranged from 6,812 MPa to 42,878 MPa [12]. It was affected largely by the source of fly ash, and the values varied in large scale. Results showed that the modulus of elasticity of the geopolymer concrete is affected by the modulus of both the geopolymer paste and the aggregate. Moreover, it was found that increasing the ratio of the activating solution to fly ash results in higher porosity and less strength and modulus of elasticity. It was also found that the mechanical properties of the geopolymer concrete are similar to that of ordinary

concrete. Furthermore, the resistance of geopolymer concrete against corrosion due to sulfuric acids was found to be considerably greater than it for the OPC concrete. Therefore, the study concludes that geopolymer concrete is preferable in the structures that are exposed to sulfuric salt attacks [12].

A different study was conducted by Abdul Aleem and Arumairaj [13] in an attempt to find the optimum mix of fly ash geopolymer concrete. The calculations of mix proportions resulted in using 103 kg/m^3 of Na_2SiO_3 solution, and 41 kg/m^3 of NaOH solution. The ratio of Na_2SiO_3 to NaOH used in the study was 2.5:1. The researchers used steam curing for the concrete specimens because previous studies indicated that geopolymer concrete hardens only by steam curing or curing by hot air for a minimum of 24 hours, and that water curing is not beneficial. However, Nath and Sarker [15] found that the introduction of GGBS in fly ash-based geopolymer concrete leads to compressive strength and workability similar to that of OPC concrete at low ambient temperature curing and without the need of heat curing. The results of Abdul Aleem and Arumairaj's [13] study show that geopolymer concrete performs well in terms of workability and strength. The researchers also found that increasing the amount of coarse and fine aggregates increases the bond between them and the alkaline solution, which in turn increases the compressive strength of the concrete. Similar conclusion was drawn by Temuujin et al. [21]. They concluded that the compressive strength of geopolymer concrete is affected by the strength of its binder and the bond between the binder and the aggregate. They also concluded that geopolymer binder can develop a good bond with the fine aggregate [21]. The optimum mix of fly ash-based geopolymer concrete at the end of Aleem and Arumairaj's [13] study was found to give a compressive strength of 52.44 MPa after 28 days. The ratio of the activating solution to fly ash was 0.35 [13].

Ryu et al. [22] tested the effect of the alkaline solutions on the strength of 100% fly ash-based geopolymer concrete. Coarse aggregate was not used in their mixes in order to eliminate its effect on the strength. Different molarities of NaOH were used: 6, 9, and 12 M. Moreover, the researchers studied the difference it will make if only NaOH is used as an activator, and the effect of mixing it with another activator such as sodium silicate (Na_2SiO_3). Results showed that a higher molarity of NaOH increases the compressive strength; furthermore, it results in a higher early compressive strength due to a sudden geopolymerization reaction. 12 M NaOH gave

the highest compressive strength of 46 MPa at 56 days. The reason behind this was referred to the higher breakage of the glassy chain of fly ash as more alkalinity is provided when molarity increases. It was also found that a combination of the NaOH and Na_2SiO_3 as activating solution gave better compressive strength of 47 MPa than using one activating solution. Ryu et al. [22] also used SEM analysis to study the microstructure of the fly ash-based geopolymer concrete. The alkali solution dissolves soluble phases of fly ash which in turn releases alumina and silica from the fly ash particles surface. These phases react with the alkalis coming from the activating agent and then condense on the fly ash surface, forming the shell of alumino-silicate gel [6]. Figure 7 shows the SEM image of Ryu et al. [22] geopolymer specimen at 28 days with some particles of fly ash that did not experience the geopolymerization reaction.

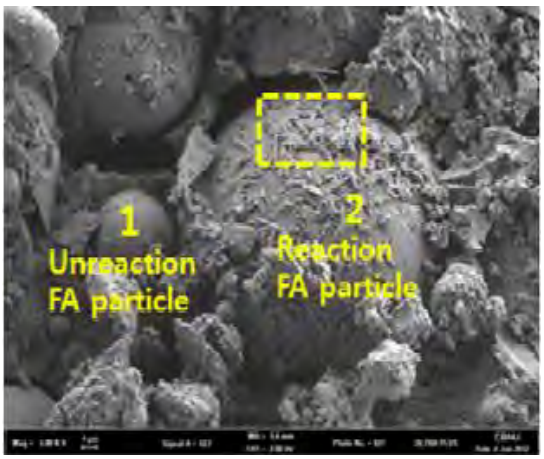

Figure 7: SEM image of fly ash based geopolymer concrete [22].

Those particles do not act as fillers, but they help in improving the strength in the long run as their surface provides a good bond between particles [22].

Ravikumar et al. [6] studied the factors that affect the compressive strength in geopolymer fly ash-based and GGBS-based concretes. They used only 8 M NaOH as activating solution for fly ash-based and GGBS-based geopolymer concrete mixes. They mixed first the fly ash/or GGBS with fine and coarse aggregate for 2 minutes, and then, the activating solution was added to the mix. After that, the whole material was mixed for another 4 minutes in the case of fly ash, and for 2 minutes for the GGBS mix. That was due to the faster setting time of the GGBS-based geopolymer concrete. The researchers demolded the specimens after 24 hours and cured them using heat curing at 60°C and 75°C for 12, 24, and 48 hours. Activating to binder ratio

used was 0.4. Ravikumar et al. [6] tested different quantities of binder by volume of fly ash and GGBS and found that the optimum amount of fly ash binder that gave the highest compressive strength was 18% by volume of concrete, and 25% by volume for GGBS concrete. Moreover, they found that when curing temperature was increased from 60°C to 75°C, significant increase in the compressive strength was recorded. In addition, when curing duration was increased from 12 to 48 hours, higher compressive strength was obtained. Figure 8 summarizes the study results.

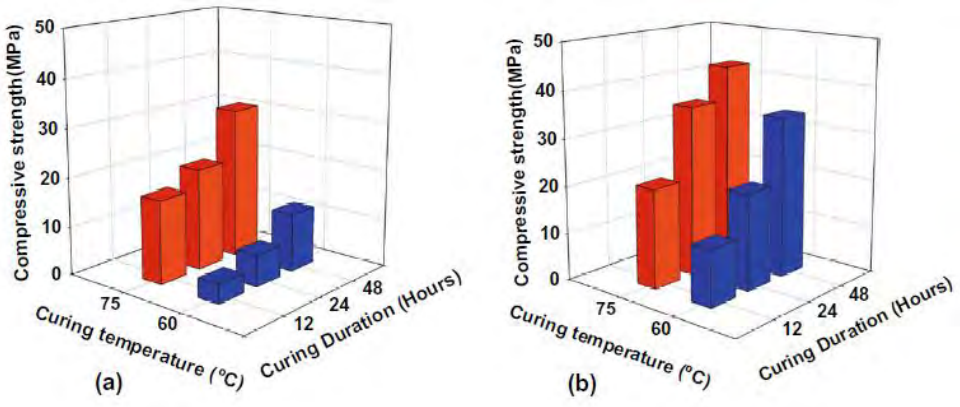

Figure 8: (a) Fly ash-based geopolymer concrete (b) GGBS-based geopolymer concrete [6].

According to Bondar [23], the compressive strength of geopolymer concrete is a function of the alkaline solutions type and concentration, curing time and temperature, amount of silicate, aluminate, and potassium/sodium in the concrete matrix. Ravikumar et al. [6] also studied the effect of activating solution to binder ratio and found that the ratio of 0.4 resulted in the highest compressive strength for both fly ash and GGBS mixes as shown in Figure 9.

They also found that GGBS geopolymer mix recorded higher compressive strength than fly ash-based geopolymer concrete. They related this to the higher binder percentage per volume of the GGBS mix, and to the property of self-cementing in GGBS which is due to containing high amount of CaO. Microstructural analysis using SEM showed that the reaction product of alkaline-aluminosilicate gel forms a shell surrounding the particles. This product was distributed more homogenously in the case of GGBS. Moreover, fly ash had more unreacted particles. However, these particles will trigger more reaction in the long term and thus higher compressive strength can be achieved then [6].

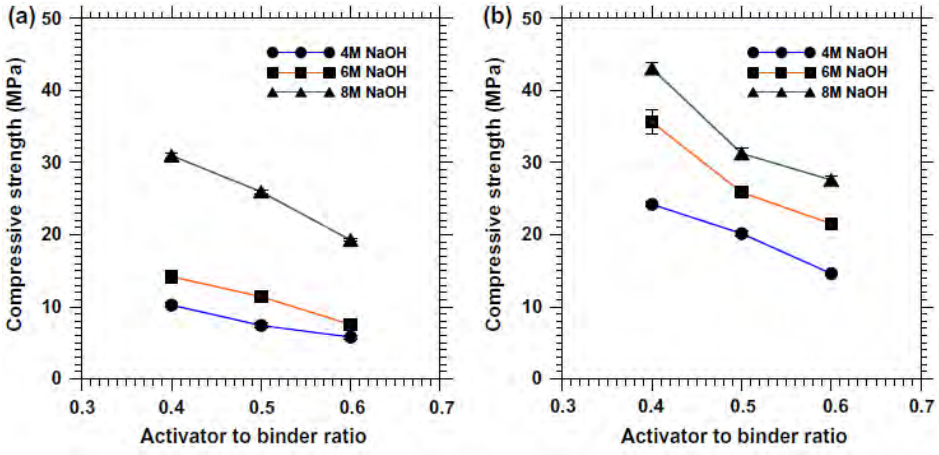

Figure 9: Effect of activating solution to binder ratio for (a) fly ash and (b) GGBS geopolymer mixes [6].

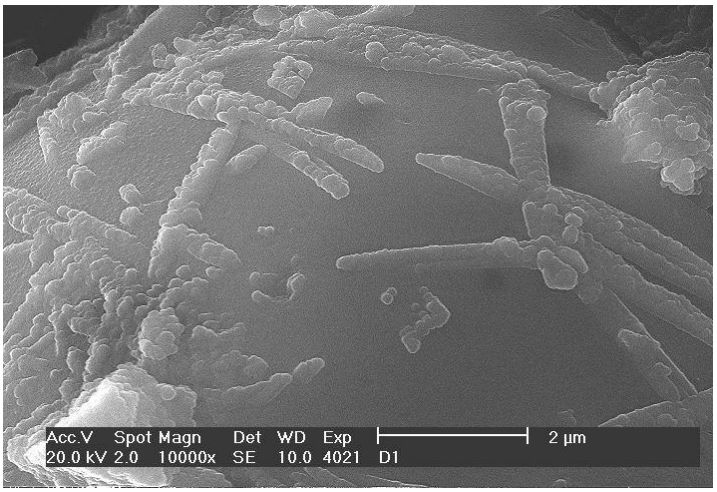

Figure 10: The initiation of geopolymer on the surface of an original fly ash particle [9].

Motorwala et al. [9] tested fly ash based geopolymer concrete with different molarities of NaOH. They used three types of alkaline solutions, NaOH, KOH and Na_2SiO_4, mixed in different ways. Oven curing was used for 24 hours. They found that increasing the temperature of the oven for curing geopolymer concrete specimens increased the compressive strength of the concrete. However, increasing the temperature beyond 80^o Celsius was not considerably beneficial. The researchers also found that fresh geopolymer concrete is stiff. This is in accordance with Okoye et al. [7], where geopolymer concrete was creating pellets while mixing. Superplasticizer was used to improve the workability of the fresh concrete. Motorwala et al [9] also found that longer curing time and higher molarity of sodium hydroxide increase the compressive strength. They concluded that the selection of aggregate type and the

grading of aggregate play an important role in the compressive strength of geopolymer concrete. Higher grading (more different sizes of aggregate present in the mix) leads to higher compressive strength. The researchers also found that sun curing can give efficient result of compressive strength, which makes fly ash-based geopolymer concrete suitable for site use in summer times in hot areas [9]. Figure 10 shows the initiation of geopolymer gel on the surface of fly ash particle found by Motorwala et al. [9].

Ravikumar et al. [6] tested the microstructure of the geopolymer concrete of two different mixes containing different percentages of GGBS and fly ash. The first mix had 10% of GGBS blended with fly ash, and the second mix had 50% of GGBS. NaOH was mixed with sodium silicate as activating solutions. SEM test revealed more compact and less porous samples for the mix with 50% GGBS. However, there were more un-reacted GGBS particles. For the 10% GGBS mix, more fly ash un-reacted particles were found at 28 days. The researchers reported that the addition of more GGBS in the geopolymer mix increases the calcium content, which as a result increases the bonding gel with the aggregate since more calcium silicate hydrate (C-S-H) is formed. Geopolymer concrete generally has less workability than normal concrete with OPC. This was explained by the more viscous materials used in the geopolymer concrete than normal concrete [6], [7]. Ravikumar et al. [6] reported stiffer and less workable concrete when more GGBS was added. This is because of the faster rate of reaction of GGBS and less sitting time. Moreover, the irregular shape of GGBS particles has a negative impact on the workability. Workability also depends on the amount of activating solution added; more solution gives higher workability [6]. Ravikumar et al. [6] reported more factors affecting the workability of geopolymer concrete such as the ambient temperature while mixing, mixing time, and moisture content of aggregate. Unlike OPC concrete, superplasticizers do not improve geopolymer concrete workability significantly according to King and Sajayan [10]. They state that increasing the amount of superplasticizer added to the concrete matrix decreases the overall strength and is not efficient in concrete subjected to elevated temperatures.

Kong and Sanjayan [10] studied the effect of elevated temperature on the performance of the geopolymer concrete, and compared it with OPC concrete

specimens. As shown in Figure 11, geopolymer compressive strength started to increase until 300 ^{o}C and then decreased gradually to a final strength of 58 MPa at 800 ^{o}C. On the other hand, OPC samples started losing strength at the instance of being exposed to high temperature, and the loss was significantly increasing until the samples lost their complete strength at 400 ^{o}C. This significant loss of strength in the OPC samples was reported to be due to the decomposition of calcium hydroxide in the concrete paste.

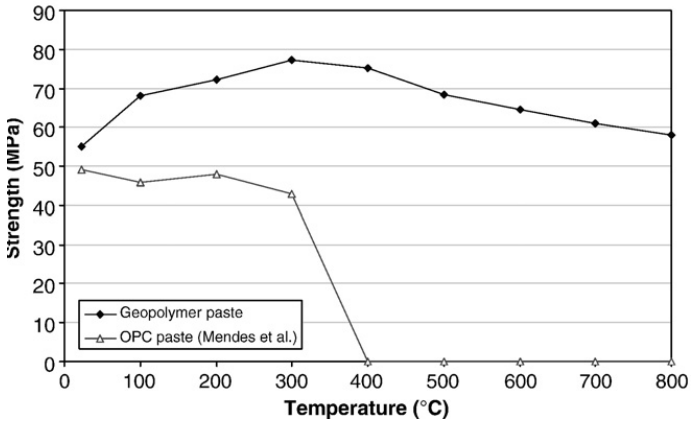

Figure 11: Comparison between strength of OPC concrete samples and geopolymer concrete samples at elevated temperatures [10].

Although geopolymer concrete recorded higher fire resistance than normal concrete, this resistance depends on a number of factors. One of these factors is the size of aggregate. Larger aggregate size (greater than 10 mm) was found to be more effective in concrete fire resistance, while samples with smaller aggregate size experienced more spalling and cracking [10].

Okoye et al. [7] tested the effect of silica fume on geopolymer concrete with fly ash. They found improvement in the compressive strength of the specimens when higher percentage of silica fume was added. However, an opposite effect on workability of the fresh concrete was observed. The same conclusion was obtained by [18]. Okoye et al. [7] were able to obtain a 28-days compressive strength of 51 MPa using 40% silica fume added to fly ash. They referred the improved strength to the high SiO_2 content available in the silica fume which increased the formation of the alumino-silicate gel [7], [20]. They also reported improvement in the flexural and tensile strengths of the concrete samples as silica fume content increased in the

matrix. Okoye et al. [7] and Bakharev [19] reported better resistance of geopolymer concrete to chemical attacks than OPC concrete since it contains finer materials, denser structure, and varied binding gels such as Na-S-H and C-S-H.

Lee et al. [18] studied the reactivity of the fly ash and slag with the alkali solution when silica fume was added as percentage substitution to those materials. They tested different types of silica fumes from different resources. The researchers concluded that generally silica fume can significantly change the chemical composition and the silicate structure of the different gels the geopolymer paste has. They also reported that the addition of silica fume to the mix decreases the reactivity of the fly ash with the alkali activator and increases it in the case of slag. They referred that to the morphology of the silica fume being more amorphous than fly ash. Alkali solution reacts more with amorphous structure such as silica fume, where fly ash particles are more crystalline. Moreover, they found that Al from the slag reacts more with silica fume than fly ash [18].

Table 1: CO_2 emission factors for different concrete production activities
Adapted from Flower and Sanjayan [5]

Activity	Emission factor	Unit
Coarse aggregate-Granite/Hornfels	0.0459	t CO_2-e/tonne
Coarse aggregate – Basalt	0.0357	t CO_2-e/tonne
Fine aggregate	0.0139	t CO_2-e/tonne
Cement	0.8200	t CO_2-e/tonne
Fly ash (F-type)	0.027	t CO_2-e/tonne
GGBS	0.1430	t CO_2-e/tonne
Concrete batching	0.0033	t CO_2-e/m^3
Concrete transport	0.0094	t CO_2-e/m^3
On site placement activities	0.0090	t CO_2-e/m^3

1.3.2 Carbon footprint evaluation of concrete. Flower and Sanjayan [5] were able to establish a factor for CO_2 emissions for each concrete production activity as shown in Table 1. The unit is equivalent-CO_2 for each ton of material, which takes

into account the global warming potential. The researchers used these factors to calculate the total CO_2 emissions for a public housing that was real proposed but not built yet in Australia.

The results of Flower and Sanjayan's [5] calculations are shown on Table 2. They multiplied the expected quantity of concrete needed in cubic meters for each construction activity by the carbon emission factor related to it. Then, the emissions from each activity were summed up to get the total CO_2 emissions resulted from the construction of the proposed structure as shown in Table 2. Calculating carbon emissions can be done prior to construction to give information on how environmentally friendly the structure will be.

Table 2: Calculations of embodied carbon emissions for a proposed structure in Australia. Adapted from Flower and Sanjayan [5]

Strength (MPa)	Structural element	Quantity (m^3)	Emission factor (t CO_2-e/m^3)	Emissions (t CO_2-e)
15	Blinding	589	0.20	119
32	Footings	489	0.24	119
32	Slabs	1948	0.27	533
40	Insitu Columns & Walls	235	0.27	63
40	Precast Walls	1067	0.33	351
			Total	1185

In general, research work on geopolymer concrete performance is still limited, and a new structural binding material needs a thorough research and more investigations. Most of the previous research work focused only on the compressive strength of geopolymer concrete; whereas durability was often ignored. Moreover, most studies focused on the fly ash or slag as the only base material for the geopolymer binder. The effect of using different reactive solids combined together on different percentages is the concern of this study. Therefore, this study developed and evaluated geopolymer concrete mixes with different percentages and combinations of reactive solids which are cementitious materials, including fly ash, silica fume, and

GGBS. Moreover, the mechanical behavior, durability, morphological investigations, and carbon footprint of geopolymer concrete mixes were evaluated and compared with normal concrete mix properties.

1.4 Significance of Research

Most of the studies on geopolymer concrete samples used the curing by steam or heat for a considerable period of time. In fact, this is considered energy intensive and is not practical to be used in site, and it may be limited to precast members. Therefore, a need for a geopolymer concrete that can be cured in ambient conditions is crucial. This concrete will have the potential to be used in site and reduce production cost and energy. Therefore, this study aims at producing geopolymer concrete with reasonable strength that is cured at ambient temperature, which can be then used in site without the need for expensive heating techniques. The effect of heat curing on strength and durability of geopolymer concrete specimens is also tested in this study. Moreover, this study utilizes different cementitious materials with different percentages to produce geopolymer concrete specimens with good mechanical behavior and durability. It aims at utilizing more waste materials in one mix other than fly ash, the material which most of the previous studies focused on. The use of these materials as a complete replacement for cement will not only reduce the amount of carbon dioxide released to the atmosphere through concrete production, but will also manage waste materials and reuse them instead of being disposed with large quantities in landfills. A greener environment with less carbon footprint, less waste materials, less need for landfills would be achieved if geopolymer concrete paste would be a binder to replace cement paste in structural concrete production.

Chapter 2: Experimental Program

Seven different concrete mixes were prepared for this study in the construction lab at the American University of Sharjah (AUS). Samples were casted, cured, and tested for fresh and hardened stage properties as illustrated in this chapter.

2.1 Materials Characterization

2.1.1 Cement and cementitious materials properties.

Table 3: Chemical composition of fly ash, GGBS, silica fume, and cement used in this study

Chemical/property	Fly ash Wt. (%)	GGBS Wt. (%)	Silica Fume Wt. (%)	Cement Wt. (%)
SiO_2 + AL_2O_3+Fe_2O_3	91.27	-	-	-
Al_2O_3	-	15.3	0.49	4.7
Fe_2O_3	-	0.7	1.49	4
SiO_2	61.86	32.9	92.98	20.5
MgO	0.86	5.9	0.57	1.8
SO_3	0.28	0.21	0.57	2.4
Moisture content%	0.06	0.71	0.46	-
LOI* %	0.83	2.1	1.8	1.5
IR**	-	0.30	-	0.34
CaO	-	41.3	0.32	64.1
S	-	0.85	-	-
Na_2O	-	0.45	0.47	0.58
Mn_2O_3	-	0.34	-	-
Cl-	-	0.01	0.04	0.02
K_2O	-	-	0.51	-
C	-	-	1.45	-
C_3A	-	-	-	5.7

*Loss on ignition
** Insoluble residue

Materials used in this study were obtained from locally based suppliers. Class (F) fly ash was used in this study. Its chemical composition which complies with the ASTM C-618 standards is presented in Table 3. GGBS was obtained from Sharjah Cement Factory. Its chemical composition complies with ASTM C 989 standard as illustrated in Table 3. Silica fume was obtained from Elkem AS, Silicon Materials®, and its chemical composition conforms to ASTM C 1240 as shown in Table 3. OPC was obtained from Sharjah Cement Factory, and its chemical composition is presented in Table 3. This table also shows other properties of the materials used to prepare the concrete mixtures used in this study.

2.1.2 Coarse and fine aggregate properties. Coarse and fine local aggregates in dry condition were used in the concrete mixes in this study. Crushed coarse aggregate was used with two different sizes (60% -by total weight- from the size 5-10 mm, and 40% from the size 10 – 20 mm). The fine aggregate consists of 60% (by weight) crushed sand and 40% (by weight) dune sand. Their properties were tested in the lab; these tests include: sieve analysis for coarse and fine aggregates according to ASTM C-136, specific gravity and water absorption of coarse aggregate according to ASTM C127, bulk density of coarse and fine aggregate according to ASTM C29, specific gravity and water absorption of fine aggregate according to ASTM C128-07, and fineness Modulus of fine aggregate. Results of these tests are shown in Table 4 and Figure 12. The results presented in Table 4 are obtained to be used in the concrete mix design explained in proceeding sections.

Table 4: Coarse and fine aggregate properties

Property	Coarse aggregate	Fine aggregate
S.G	2.66	2.54
Water Absorption (%)	1.29	1.56
Bulk Density (kg/m3)	1525	1619
Fineness Modulus	-	2.045

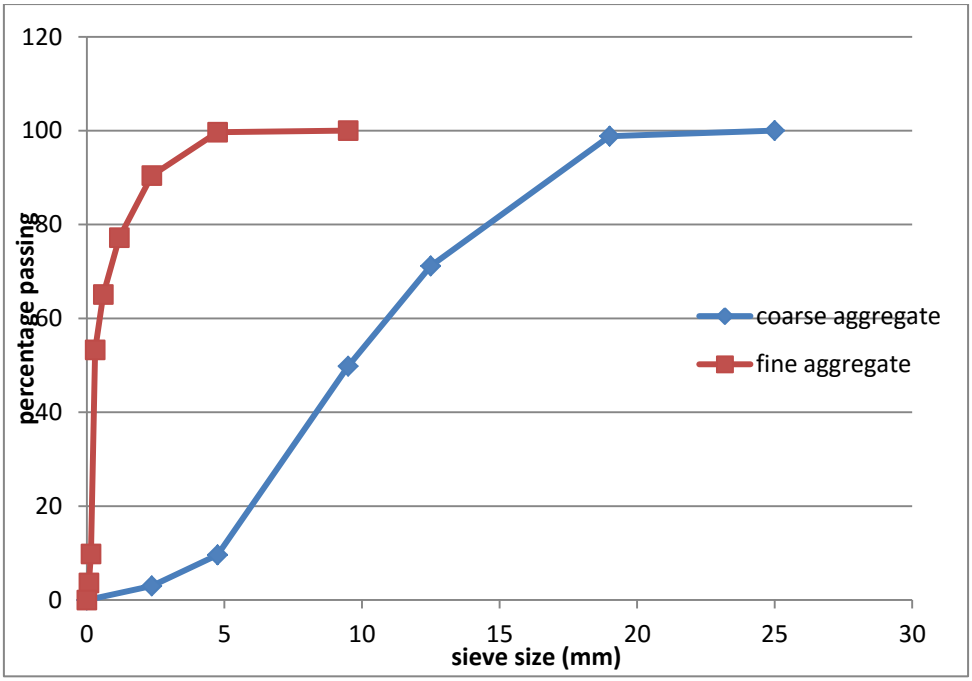

Figure 12: Coarse and fine aggregates grading.

Figure 12 shows that aggregates used in this study are well graded, since different aggregate sizes are present in the mix as the Figure shows. Glenium superplasticizer available from BASF was used in all of the mixes to enhance the workability. The amount of superplasticizer added in each mix is presented in Table 6.

2.1.3 Activating solutions. Geopolymerization process will not take place unless activating solutions are added to the reactive solids (cementitious materials) in order to activate them to perform as cement. Alkali activating solution used in this study was 10 M sodium hydroxide (NaOH) solution prepared in the lab one day prior to each mix. 99% pure sodium hydroxide pellets was dissolved in normal tap water and allowed to cool down to room temperate before being used in the mix. For each mix, a mass of 3.24 kg of NaOH pellets were dissolved in 8.11 liters of water and mixed properly to insure complete dissolution of pellets. In order to prepare 10 M of NaOH solution, knowing that the molecular weight of NaOH is 40 g/mole, 10*40*8.11*10^-3 = 3.24 kg of NaOH pellets were used in each mix. A ratio of 0.35 of activating solution to reactive solids was used in all geopolymer concrete mixes prepared in this study.

2.2 Mixture Design

High performance mix design method was used to determine the proportions of all the mixes including quantities of the cementitious materials, water, coarse and fine aggregates, and admixtures according to ACI 211-1. This method is based on the absolute volume method of mix design and is a combination of mathematical calculations and empirical results proposed by [24].

Seven different concrete mixes were made in this study as shown in Table 5. Six of them were geopolymer concrete mixes with different ingredients and different percentages. These mixes were obtained, and specimens were prepared and tested for various tests against normal concrete mix specimens that contain only cement with a w/c ratio of 0.35. A base concrete mix design for normal concrete with cement was made, and quantities were calculated and obtained and then adjusted for each of the geopolymer concrete mixes based on their component percentages. The quantities per one cubic meter for all the concrete mixes are presented in Table 6. Wherever silica fume was added, its amount was fixed to 15% of the total weight of reactive solids as it is stated by [17] that this percentage is an optimum in a concrete mix. Moreover, it was fixed in order to decrease the number of variables among the geopolymer concrete mixes. Other percentages were selected randomly to observe the effect of different combinations and then choose an optimum mix that gives the best results among the proposed mixes.

Table 5: Concrete mixes of this study

Mix number	Cement%	Fly ash%	GGBS%	Silica fume%
CM	100	-	-	-
F100	-	100	-	-
G100	-	-	100	-
F80-G20	-	80	20	-
F70-G15-S15	-	70	15	15
F85-S15	-	85	-	15
F15-G70-S15	-	15	70	15

In all the mixes prepared in this study, the quantities of water, coarse and fine aggregates, and sodium hydroxide solution were fixed in order to eliminate the effect of changing their quantities. CM is the normal concrete control mix which all the mixes were compared with since it has only cement and none of the supplementary materials were used in it. The other mixes are geopolymer concrete mixes which had cementitious materials that replaced cement totally, and it was not used at all. The percentages shown in Table 5 are percentages of the cementitious materials in the geopolymer concrete mixes by weight of total binder (reactive solids).

Table 6: Mix proportions of this study in kg/m^3

Materials	CM	F100	G100	F80-G20	F70-G15-S15	F85-S15	F15-G70-S15
Water	154	154	154	154	154	154	154
Coarse aggregate (total)	1036.5	1036.5	1036.5	1036.5	1036.5	1036.5	1036.5
Dune Sand	319.5	319.5	319.5	319.5	319.5	319.5	319.5
Crushed Sand	479	479	479	479	479	479	479
Cement	392	0.0	0.0	0.0	0.0	0.0	0.0
Fly Ash	0.0	392	0.0	314	274.5	333	59
Silica Fume	0.0	0.0	0.0	0.0	59	59	59
Slag	0.0	0.0	392	78.5	59	0.0	274.5
NaOH solution	0.0	137	137	137	137	137	137
Superplast.	2.5	2.5	2.5	2.5	2.5	2.5	2.5

2.3 Mixing Process

In the mixer, first the coarse aggregate of both sizes was added and mixed with water for two minutes to reduce the amount of dust released. Following, the quantity of sand was added and mixed for another two minutes until the coarse and

fine aggregates were mixed homogenously. Then, the quantity of the reactive solids was added and then followed by the amount of sodium hydroxide solution. The mix was let to rotate for five minutes to ensure that the reaction takes place between the reactive solids and the activating solution. In the case of GGBS mixes, mixing time was slightly less due to the fast setting time of the GGBS compared to fly ash [6]. Superplasticizer was added at the end with any extra water the mix needed to enhance workability and ease mixing. In general, geopolymer concrete mixes were harsh and stiff, and almost all of them needed little extra water to be able to mix and pour. Furthermore, they were creating balls while mixing, which were reduced by the addition of water. The same observation was reported by [9] and [7].

2.4 Specimens Preparation

After preparing molds, concrete was casted in specimens and tested in the lab for several properties as discussed in details in the proceeding sections. Each mix had 5 small cylinders with diameter 100 mm and height 200 mm, 3 large cylinders with diameter 150 mm and height 300 mm, 3 beams (500*100*100 mm), and 6 cubes (100*100*100 mm). A total of 102 specimens were casted; these include 30 small cylinders, 18 large cylinders, 18 beams, and 36 cubes. Specimens were casted in three layers and compacted using a tamping rod 25 blows according to ASTM C192, and then the mechanical vibrating table was used to release air bubbles. Proper compaction was needed to prepare the specimens; however, it was not an easy task due to the stiff nature of the geopolymer concrete mix.

2.5 Curing Systems

Previous studies on geopolymer concrete state that it cannot be hardened unless cured by elevated temperature or by hot steam curing. However, for this investigation, specimens were cured under the sun for 7 days and then put inside the room at ambient temperature. They were not sealed because there was remaining excess water in the paste, and the specimens remained wet for a considerable period of time. After 7 days of casting, specimens were de-molded and kept at ambient temperature. However, on the same day, two cubes from each mix were put in the laboratory oven for heat curing at 75^{o} C for 24 hours in order to investigate the effect of heat curing on the properties of the concrete specimens. These oven-cured

specimens were tested for compressive strength at 28 days. The other specimens were tested at 7 and 28 days of casting date. A trial mix was made in this study to also test the efficiency of water curing for the geopolymer concrete specimens. This trial mix was made on a randomly selected mix which is mix F85-S15. The specimens of this mix were put in water tank for 7 days.

2.6 Testing of Concrete

2.6.1 Testing events. Testing events and samples are summarized in Table 7.

Table 7: Testing events and concrete specimens for each mix

Testing Events	Specimens			
	Cubes	Beams	Large cylinders	Small Cylinders
7-day	Compressive strength	-	-	-
28-day	Compressive strength	Flexural strength	Elasticity Modulus	Tensile strength & RCPT

After 7 days of concrete casting, compressive strength of concrete cubes was tested as an indication for the early strength of concrete, and to know how much strength was gained at the late age of 28 days.

2.6.2 Testing of fresh concrete.

2.6.2.1 Slump test. All concrete mixes were tested for slump using slump test according to ASTM C143-98 procedure which evaluates its workability as shown in Figure 13, and the results were compared to the slump of the control mix.

2.6.2.2 Air content test. Air content of the fresh concrete was tested for all mixes according to ASTM C231-97 pressure method test as shown in Figure 14.

Figure 13: Slump test setup.

Figure 14: Air content test apparatus.

2.6.2.3 Density of fresh concrete. The density of the fresh geopolymer and normal concrete mixes, in kg/m^3, was calculated by dividing the mass of the fresh concrete over the volume as shown in equation (2)

$$D = \frac{m}{V} \qquad (2)$$

where m is the mass of the fresh concrete in kg, and V is the volume in m^3.

2.6.3 Testing of hardened concrete

2.6.3.1 Compressive strength test. Compressive strength of concrete cubes (100*100*100 mm) of all the mixes was conducted at 7 and 28 days according to BS EN 12390-3:2009 as shown in Figure 15. Cubes were placed at the center of the compression machine and placed in a way the load was applied at a direction perpendicular to the casting direction. Constant load was applied until failure. Results were obtained and averaged for each event. Failure plane (whether in the concrete paste or in the aggregate) was also investigated. This test was done on both oven cured and ambient temperature cured cubes at 28 days. Results of this test are illustrated in the next chapter.

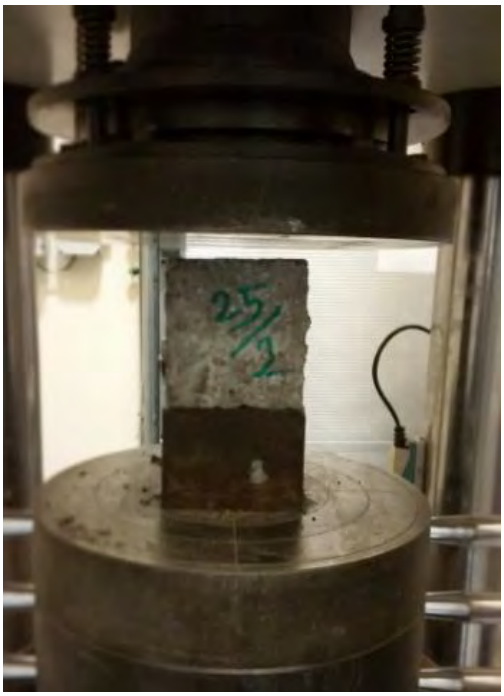

Figure 15: Compressive strength test setup.

2.6.3.2 Tensile strength test. This test was conducted on concrete cylinders having a diameter of 100 mm and height 200 mm at the age of 28 days according to ASTM C-496. This test was done by applying a compressive force along the length of

the cylindrical concrete specimen at a constant rate until failure. This load produces tensile stresses on the plane where the applied load is. Failure due to tension occurs instead of compression failure because the plane of load application is under triaxial compression. Therefore, it can withstand higher compressive stress than uniaxial compressive strength test would give. The cylinder was placed horizontally in the testing machine where the load was applied along its length as shown in Figure 16. This test was applied on ambient temperature cured specimens only. Three results of the tensile strength were obtained for each mix and averaged. The results of this test are illustrated in the next chapter.

Figure 16: Tensile strength test setup.

2.6.3.3 Flexural strength test. Flexural strength of concrete beams having the dimensions of (500*100*100 mm) was measured using center point loading test at the middle of the beam according to ASTM C 293 as shown in Figure 17. The center point loading was applied at the center of the beam, and the reactions were placed at 10 cm from the edge of the beam. Constant rate loading was applied at the center of the beam until breaking.

Flexural strength can be determined through calculating the modulus of rupture (f_r) of the concrete beam using Equation (3), where P is the maximum applied

load in (N), L is the span length of the beam in (mm), b is the average width of the beam in (mm), and d is the average depth of the beam in (mm).

$$f_r = \frac{3PL}{2bd^2} \qquad (3)$$

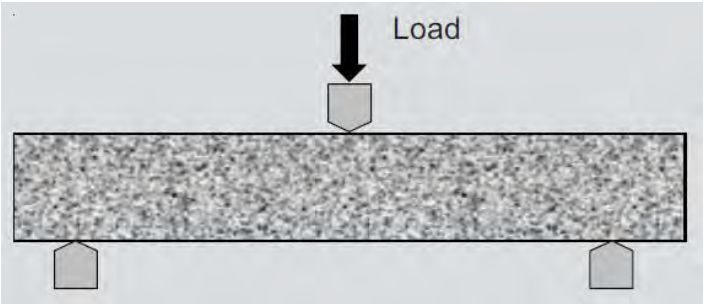

Figure 17: Center-point-loading test for concrete beams flexure.

This test was conducted on three beam specimens of each mix at 28 days. Results were obtained and averaged as illustrated in the next chapter.

2.6.3.4 Modulus of elasticity test. This test was conducted, according to ASTM C469 test method, on 28 days aged concrete cylinders. These cylinders had a diameter of 150 mm and a height of 300 mm. Modulus of elasticity was obtained using stress-strain graphs as shown in Figure 18.

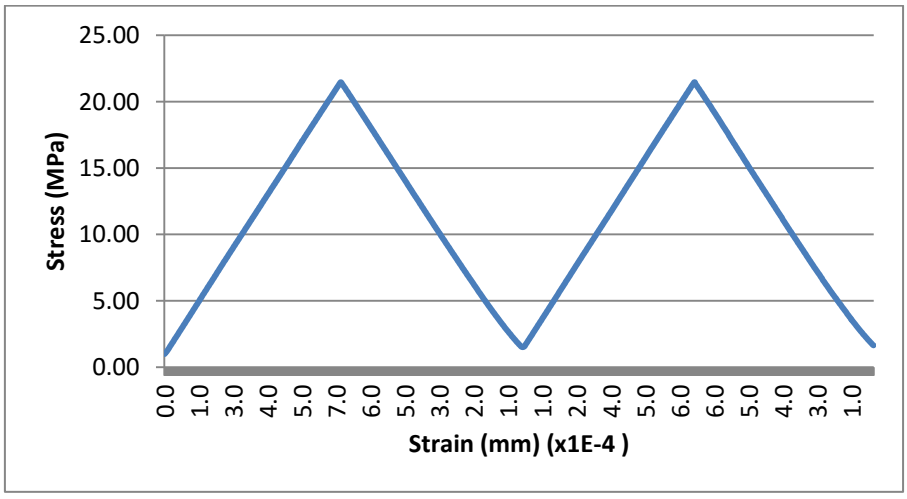

Figure 18: Stress vs strain graph by the testing machine.

Bonded strain gauges were placed around the diameter of the concrete cylinder as shown in Figure 19. These gauges read the deformation in diameter of the

specimen. A constant compressive load was applied longitudinally on the concrete cylinder. The load was applied twice as shown in Figure 18, where the first load was for calibration of the strain gauges. The computer recorded the stress and strain of the specimen till failure and calculated the value of the elasticity modulus using the ratio of the stress to strain from the graph in the stress range from 0 to 40% of the ultimate load.

Figure 19: Modulus of elasticity test setup.

2.6.3.5 Rapid chloride penetration test. In order to evaluate the durability and the resistance of geopolymer concrete against harsh environmental attacks, rapid chloride permeability test was conducted on concrete specimens according to ASTM C1202. This test measures the penetration of chloride into concrete specimen as a simulation of harsh chloride environment through measuring the electrical connectivity of the concrete. The higher the chloride penetration in the concrete specimen, the higher the porosity of the specimen is, and the lower is its resistance to environmental attacks. Concrete specimens of 100 mm diameter and 50 mm thickness were placed between two electrical poles; each pole is represented by solution reservoir. One of them is sodium chloride (NaCl) solution with 3% NaCl by weight; whereas, the other one is 0.3 M sodium hydroxide (NaOH) solution. In each reservoir,

there is a stainless steel mesh that is in contact with the specimen. To prepare the specimens, the cylinders casted for this study were cut using the sow-cut machine in the laboratory for the desired mentioned dimensions. Then, the samples were incubated in a chamber (see Figure 20) that was connected with a vacuum pump through a hose for 3 hours to ensure removal of all air inside the chamber. After that, the pump was removed and replaced by a distilled water container. The water pumped fast through the hose to the chamber due to difference in pressure as shown in Figure 21. After the specimens were submerged completely in distilled water, the hose was connected again to the pump for another hour to ensure no air entered in the chamber. The specimens were then kept in distilled water for 18 hours. Following, the specimens were removed from water and put between the two electrical poles described earlier. This system was then exposed to a 60Volt electrical voltage for six hours as shown in Figure 22.

Figure 20: RCPT samples incubated in vacuum chamber.

Figure 21: Distilled water going inside vacuum chamber due to pressure difference.

Figure 22: RCPT computerized system.

The computer reads the value of the current being transferred through the specimen and gives a value of the charge in Coulombs. This is the measure of the permeability of the concrete against chloride penetration. The penetration was categorized from negligible to high, based on the value of the charge (Coulombs) using Table 8. RCPT results and analyses are illustrated in the next chapter.

Table 8: Rapid chloride permeability measure based on charge penetrated
Adapted from Joshi & Chan [25]

Chloride permeability	Charge (Coulombs)	Type of concrete
High	> 4000	High w/c ratio (>0.6) conventional Portland cement concrete
Moderate	2000-4000	Moderate w/c ratio (0.4-0.5) conventional Portland cement concrete
Low	1000-2000	Low w/c ratio (<0.4) conventional Portland cement concrete
Very low	100-1000	Latex-modified concrete, internally sealed concrete
Negligible	< 100	Polymer-impregnated concrete, polymer concrete

2.6.3.6 Scanning Electron Microscopy (SEM). The microstructural analysis of concrete specimens has been investigated widely in research to study the morphology of concrete, the chemical reaction products, particle shape and distribution, confinement and the micro-cracks. In fact, a great deal of the macrostructural behavior of concrete can be explained by its microstructural properties. For example, the level of compactness of the geopolymer concrete can be seen in SEM images, where strength can then be related to the extent the concrete is porous [22].

In this study, SEM and EDS were carried out to study the effect of adding different reactive solids on the morphology and chemical composition of geopolymer concrete. Moreover, the test was performed to study the effect of heat curing the specimens on their microstructure. The morphology and microstructure of the geopolymer concrete specimens at the age of 28 days were evaluated in this study using a scanning electron microscope (SEM) that is shown in Figure 23.

Figure 23: Scanning electron microscope available at the laboratory.

Thin slices of concrete with a diameter of almost 10 mm and thickness of 5 mm were cut out from both oven cured and ambient cured concrete cubes. The slices were taken from the middle of the specimens to ensure being representative. Following, a plastic coating was applied on the samples to make it easier to deal with them, and to fill any air voids in the concrete specimens. Then, the resulted thin sections such as the ones in Figure 24 were grinded in the laboratory using the grinder machine shown in Figure 25 and polished using diamond polishing as shown in Figure 26. Grinding and polishing are essential steps to get flatter and smoother surface with no cracks in order to get clearer SEM pictures. The concrete samples were then taken to the SEM machine for analysis.

Figure 24: Concrete thin sections prepared for SEM with plastic coating.

Figure 25: Sample grinding machine.

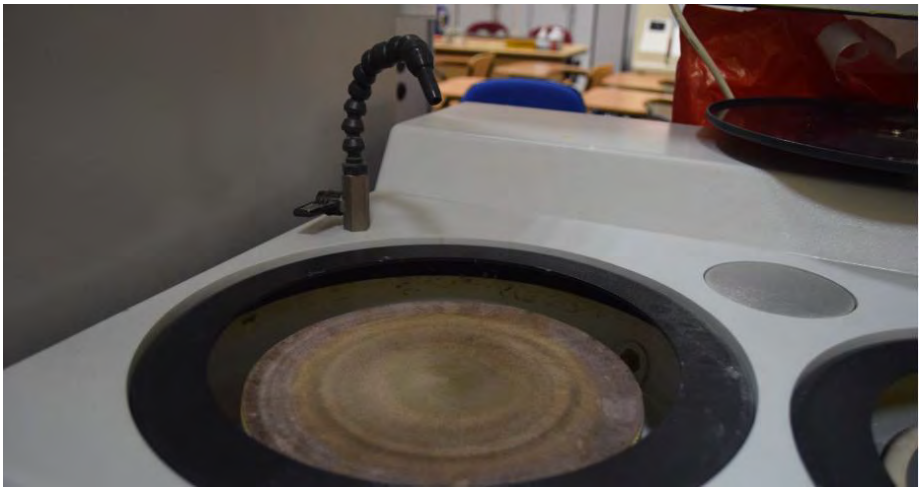

Figure 26: Diamond polishing.

The machine in Figure 23 subjects a nano-beam of electrons to the sample to scan it with an accelerating voltage up to 30 kV. The sample reflects these electrons in three groups: backscattered electrons which are of high energy, secondary electrons with low energy, and auger electrons which are electrons with low energy and excited by some atoms [26]. In this study, backscattered electrons mode was used to get the pictures of the microstructure of the specimens. The machine was connected to a computer that shows the image with magnification up to 1,000,000x. X-ray analysis on the scanned specimens was also conducted in order to specifically identify the chemical components of selected areas of the specimen and their participation in the geopolymerization reaction using Energy Dispersive Spectroscopy (EDS) feature of

the SEM machine. SEM and EDS results of the scanned specimens are illustrated in the next chapter.

2.6.4 Sustainability of concrete mixes.

2.6.4.1 Evaluation of carbon emissions. In this study, the embodied carbon dioxide of each mix prepared was calculated by summing up the carbon emissions released from the production of each of the ingredients used to prepare the geopolymer concretes including the aggregates and the paste. Factors proposed by Flower and Sanjayan [5] were used to calculate the embodied carbon emissions for the geopolymer concrete mixes according to the quantities of materials each mix contained based on the mix design. These factors, which are adapted from [5], are shown in Table 9.

Table 9: Embodied carbon dioxide emission factors

Activity	Emission factor (kg CO_2-e/kg)	Source
Coarse aggregate	0.0050	[28]
Fine aggregate	0.0139	[5]
Cement	0.8200	[5]
Fly ash (F-type)	0.027	[5]
GGBS	0.1430	[5]
Silica Fume	0.014	[31]
NaOH	1.915	[30]
Concrete batching	0.0033	[5]

Vares and Ha¨kkinen [27] point out that carbon emissions and energy consumption based on concrete production are highly dependent on the component choice and the concrete design. Since the aggregate used in this study was not specified as granite or basalt, another source of information was needed to get the factor of carbon emissions for a general type of aggregate. This factor was adapted from Hammond et al. [28] where they applied Life Cycle Assessment (LCA) to obtain these factors. This type of assessment depends on collecting data about the

environmental impact of a product from the stage of extraction to the end of the production lifetime; i.e, any process emits carbon until the product leaves the factory [29]. Their factors were based on world-wide averaged data. The coarse aggregate factor was averaged for a general type of aggregate used in the concrete mix. The factor of the carbon emissions arising from the production of the NaOH pellets was adapted from Turner and Collins [30]. Table 9 shows the factors of equivalent CO_2 emissions in kg per kg of concrete ingredient used in the mix of this study. CO_2 equivalent is a unit to measure the footprint of carbon dioxide, taking into account its global warming potential due to the emission of methane or nitrous from the same process or fuel [5]. Sources from where these factors are derived are shown in Table 9.

Other sources of carbon emissions in a concrete production such as transportation and placement activities were not considered in this study as they do not differ whether the concrete being used is normal or geopolymer. The purpose of this exercise is to show the potential benefits of using geopolymer mixes in reducing the carbon footprint. The results of the calculations are illustrated in the next chapter.

Table 10: Cost of individual concrete component in AED/unit

Material	Price (AED/unit)
Cement (per ton)	220
Water (per m^3)	10.56
Fly ash (per ton)	350
GGBS (per ton)	220
Silica Fume (per ton)	1000
Coarse aggregate (per m^3)	29.5
Dune sand (per m^3)	22
Crushed sand (per m^3)	30
NaOH pellets (per kg)	5.4
Superplasticizer (per liter)	1.5

2.6.4.2. Economics of concrete mixes. An economic feasibility analysis was conducted through calculating the cost required to prepare 1 m^3 of each mix in this study in terms of AED in UAE. The costs per unit of the individual components used in the concrete mixes of this study are presented in Table 10. These costs were collected based on site investigations at UAE market, and were used to calculate the total cost of each concrete mix as illustrated in the next chapter.

Chapter 3: Results and Discussions

3.1 Results of Fresh Concrete Testing

Slump test and air content evaluation were conducted on the fresh concrete of all geopolymer mixes and the control mix. Results of these tests are shown in Table 11.

Table 11: Results of slump, air content, and density tests

Test	CM	F100	G100	F80-G20	F70-G15-S15	F85-S15	F15-G70-S15
Slump (cm)	6.0	1.0	0.0	0.0	3.0	0.0	0.0
Air content (%)	2.0	3.3	3.8	3.0	3.0	3.1	3.5
Density (kg/m^3)	2493	2116	2249	2349	2361	2370	2196

The results of the slump test show that the geopolymer concrete mixes have very low slump and sometimes no slump (0.0 cm) when compared to the control mix CM. This was observed during mixing and casting as these two processes were hard to manage due to the stiffness of the geopolymer concrete mixes. It was also noticed that the addition of more GGBS in the mixes decreased its workability as it is clear in mix G100 and F15-G70-S15, which contain high amount of GGBS and have no slump. This was also observed in the literature by [15], [6], [9], and [7]. Mix F70-G15-S15 that has small amount of GGBS (15%) gave a better slump than the rest of the mixes as shown in Table 11. However, adding more superplasticizer to the mix was ineffective in increasing the slump because the mix was becoming more sticky and viscous when extra superplasticizer was added. This was due to the viscous nature of the geopolymer mix ingredients such as the alkaline solution of NaOH. Other ways to improve the workability of the geopolymer concrete than adding extra superplasticizer can be used. One of these ways could be increasing the amount of alkaline solution used in the mix [15].

In general, mix F70-G15-S15 which has 70% fly ash, 15% GGBS and 15% silica fume gave a better slump among all the geopolymer concrete mixes prepared in this study. The last mix, which is mix F15-G70-S15 was extremely inefficient in terms of mixing and casting and gave very low quality specimens which were full of large voids as shown in Figure 27. Therefore, this mix was discarded and excluded from the hardened concrete testing stage.

Figure 27: Very stiff geopolymer mix F15-G70-S15.

The air content test shows similar values of the geopolymer concrete mixes, ranging from 3.0% to 3.8%. It is considered high air content compared to the control mix as shown in Table 10. This indicates that geopolymer concrete is more porous.

The results of density calculations show that geopolymer concrete mixes have less density than the normal concrete mix, which means they are lighter than the normal concrete mix. The results also fall within the range obtained by [12] for geopolymer concrete density.

3.2 Compressive Strength Test Results

Results of the compressive strength test of concrete cubes of this study at 7 days and at 28 days are shown in Table 12. The values of the 28 days compressive strength shown in the table are averaged of 3 cubes in the case of normal (ambient) curing and 2 cubes for the heat (oven) curing.

Table 12: Compressive strength test results at 7 and 28 Days

Mix No	7 days compressive strength (MPa)	28 days compressive strength-Ambient curing (MPa)	28 days compressive strength- Heat curing (MPa)
CM	58	60	-
F100	0.9	4	5
G100	28	36	32
F80-G20	13	19	33
F70-G15-S15	2	7.5	12
F85-S15	4	10	20

The 7-days compressive strength of the geopolymer concrete mixes compared to the control mix (normal concrete) of this study shows that the specimens were still gaining strength during this period (from 7 to 28 days). Their strengths are considered relatively low compared to the control mix. However, mix G100 with 100% GGBS has the highest compressive strength at the age of 7 days and 28 days among the geopolymer concrete mixes of this study. The addition of GGBS in the geopolymer concrete mix increased the strength as illustrated in Table 12 and in Figure 28.

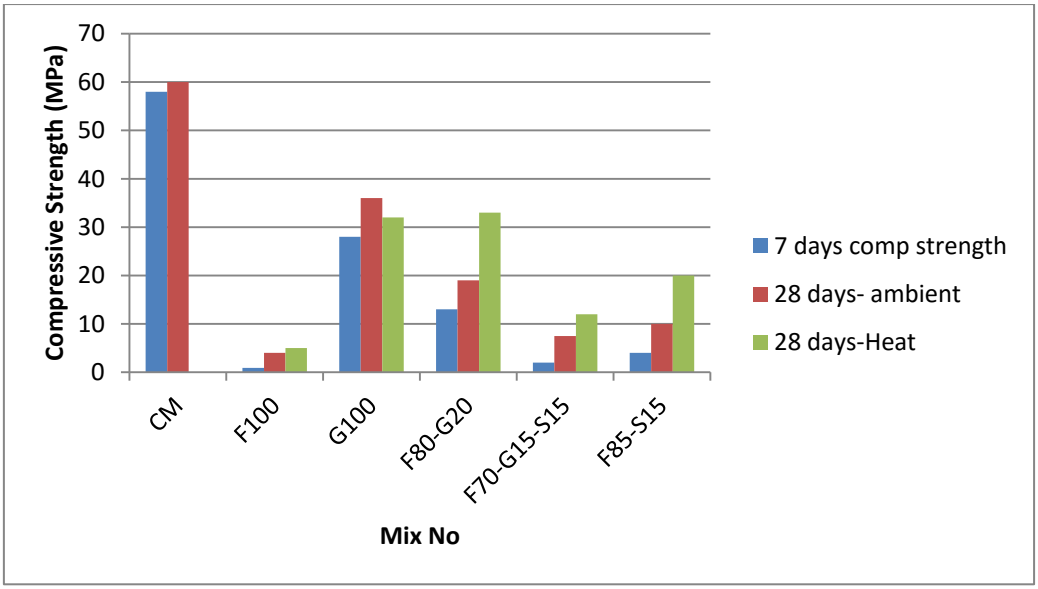

Figure 28: Compressive strength test results.

Furthermore, the early strength increased when higher GGBS amount was added. The mix F70-G15-S15 had a 7-days compressive strength that represents 26% of its 28 days strength. When higher GGBS was added in mix F80-G20, the ratio increased to 67.8% of the late strength. The ratio increased further in the mix G100 to be 78% of the late strength. It is also clear that 100% fly ash mix (F100) recorded the lowest compressive strength among all mixes. In general, mix G100 recorded the highest early and late compressive strength among all other geopolymer concrete mixes in this study without the need for heat curing as presented in Table 12 and Figure 28.

In addition, it can be seen from Table 12 that when high amount of fly ash was used, the early strength was low, and the mix did not gain enough strength at 28 days as well. This means that fly ash either needs more time than 28 days to complete reaction or does not contribute much in the formation of the geopolymer gel as GGBS does. As reported by [15], the reason behind higher strength when increasing GGBS amount in the geopolymer concrete mix is that it contains higher amount of calcium than fly ash. This makes the mix able to produce more calcium silicate gel besides the alumino-silicate one. The addition of silica fume was inefficient as shown in the Table 12, which contradicts with [7].

Figure 28 also shows that heat curing was efficient for almost all mixes, and the percentage increase in strength for oven cured specimens was in the range of 30-

99%. However, the strength of mix G100 was not affected by heat curing as shown in Table 12. This indicates that heat accelerated the rate of the reaction of almost all the geopolymer concrete mixes which as a result increased the rate of strength gain.

The failure shape was satisfactory in all the mixes cubes under compression test according to BS EN 12390-3:2009 as shown in Figure 29. Equal breaking from the sides towards the center was noticed as the figure shows. The failure plane in the geopolymer mixes in early age of 7 days was detected to be in the geopolymer paste, which indicates weak bond between the aggregate and the concrete paste. However, at the age of 28 days, the failure plane in almost all specimens was in the aggregate and the paste together which indicates that aggregate at late age of curing was able to carry load and increase the compressive strength of the specimens.

Figure 29: Failure shape of geopolymer concrete cube under compression.

As mentioned in earlier sections, a trial batch from mix F85-S15 was selected to be water cured to check the efficiency of water curing in geopolymer concrete specimens. A compressive strength test was conducted for these specimens and results are shown in Table 13. A comparison between the water cured and the ambient cured specimens of the same mix (mix F85-S15) can be seen in Figure 30.

Table 13 and Figure 30 show that water curing is inefficient for geopolymer concrete specimens. The failure plane was noticed to be in the binder of the geopolymer concrete mix as Table 13 shows.

Table 13: Compressive strength test results for water cured trial mix F85-S15

Test period	Compressive Strength (MPa)	Failure Plane
7 Days	0.3	Binder
28 Days	4	Binder

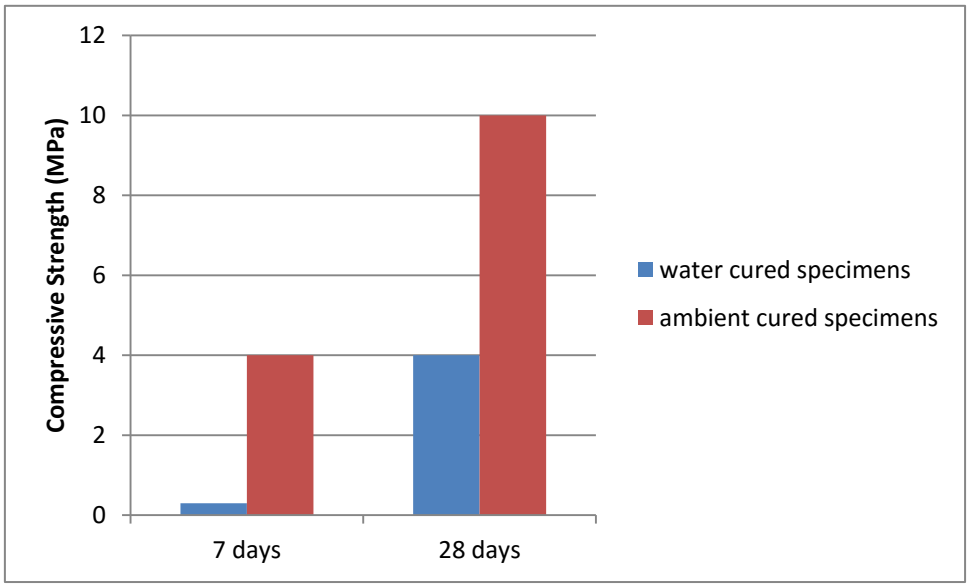

Figure 30: Compressive strength of water cured vs. ambient cured specimens of mix F85-S15.

3.3 Tensile Strength Test Results

The results of this test are the average of three testing cylinders for each mix. As shown in Figure 31, mix G100 has the highest tensile strength (2.8 MPa) among all mixes in this study. It has a tensile strength even higher than the control mix by 12% as Figure 31 shows.

All the mixes specimens had a satisfactory shape of failure after the tensile test according to ASTM C-496. The specimens were broke longitudinally into two equal halves as shown in Figure 32.

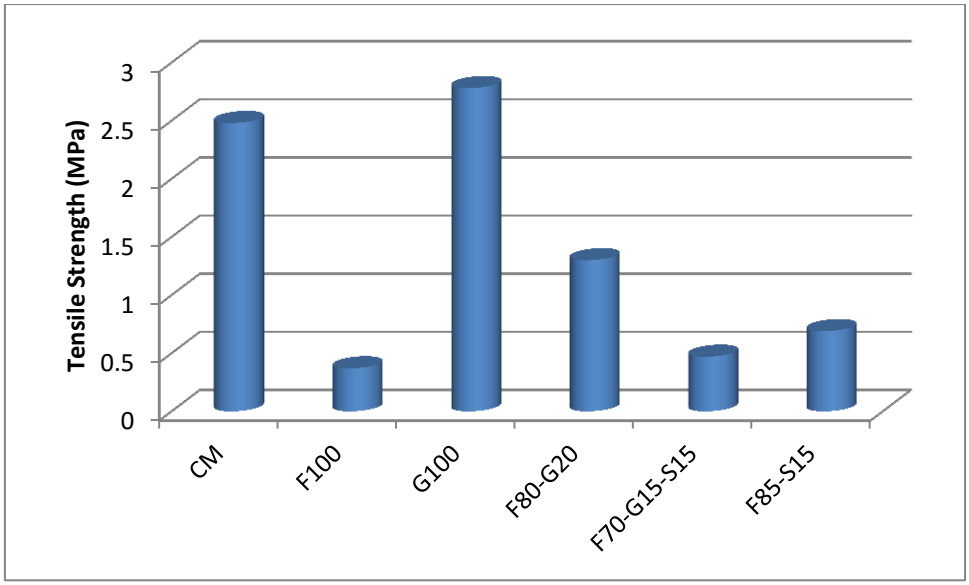

Figure 31: Tensile strength test results.

Figure 32: Failure of geopolymer concrete cylinder under tensile test load.

3.4 Flexural Strength Test Results

The flexural strength, represented by the modulus of rupture (f_r), was found using equation (3). Knowing the dimensions of the beam (specified earlier), load at failure for the testing beams recorded by the test machine was plugged into equation

(3). For example, one of the beams of mix F100 has a load at failure of 3.4 kN. Therefore, the modulus of rupture will be as follows by applying equation (3):

$$f_r = \frac{3*3.4*500}{2*100*100^2} = 0.0026 \frac{kN}{mm^2} = 2.6 \text{ MPa}$$

The results of the calculations of the flexural strength of testing concrete beams according to ASTM C 293 are summarized in Figure 33. For each mix, the value of the flexural strength is the average of three testing beam strengths.

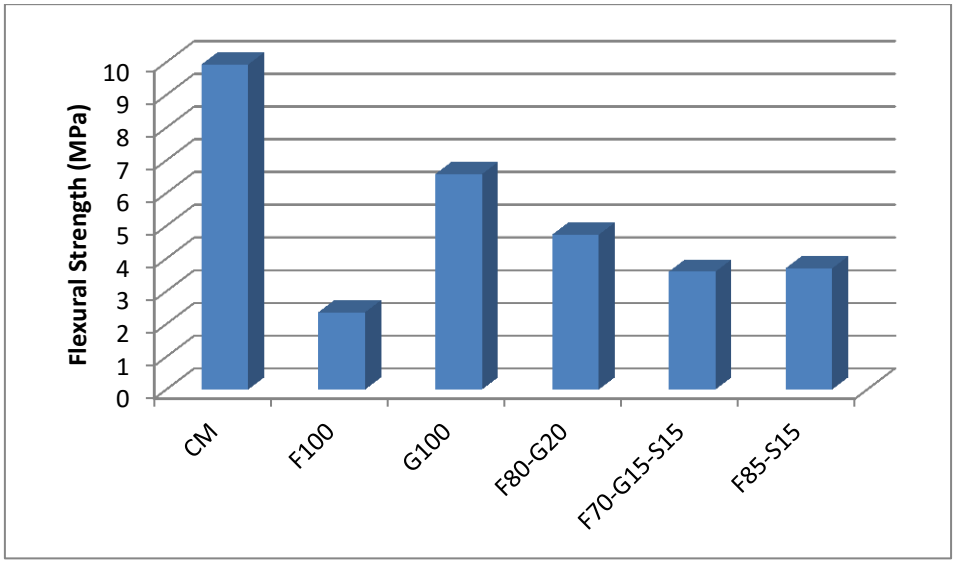

Figure 33: Flexural strength test results.

As shown in Figure 33, the flexural strength of mix G100 is the closest to the normal concrete mix. Mix G100 recorded the highest flexural strength among all the geopolymer concrete mixes with a value of 6.6 MPa.

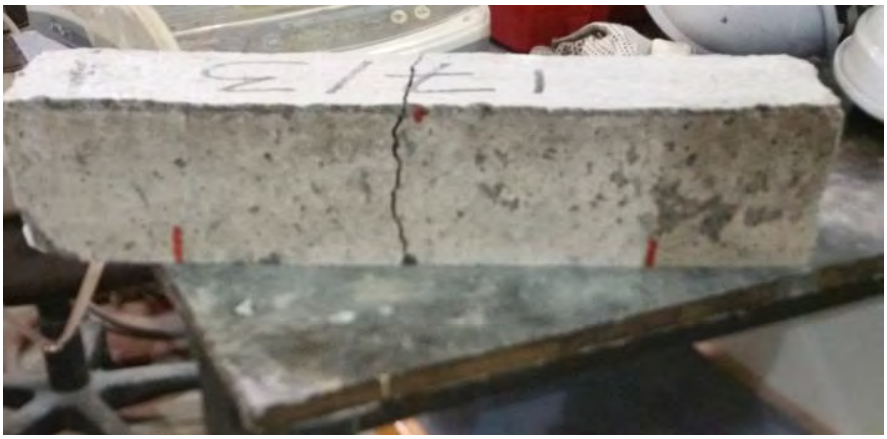

Figure 34: Failure of normal concrete beam after flexural strength test.

Figure 35: Failure of geopolymer concrete beam after flexural strength test.

Figure 35 shows a geopolymer concrete broken beam under flexural strength test. Comparing it to Figure 34 of the control mix beam failure, the crack of the geopolymer concrete beam is not exactly a pure flexural crack. However, some shear failure is noticed due to the crack having almost 45^{o} angle. Same failure shape was noticed in all the geopolymer concrete beams of this study.

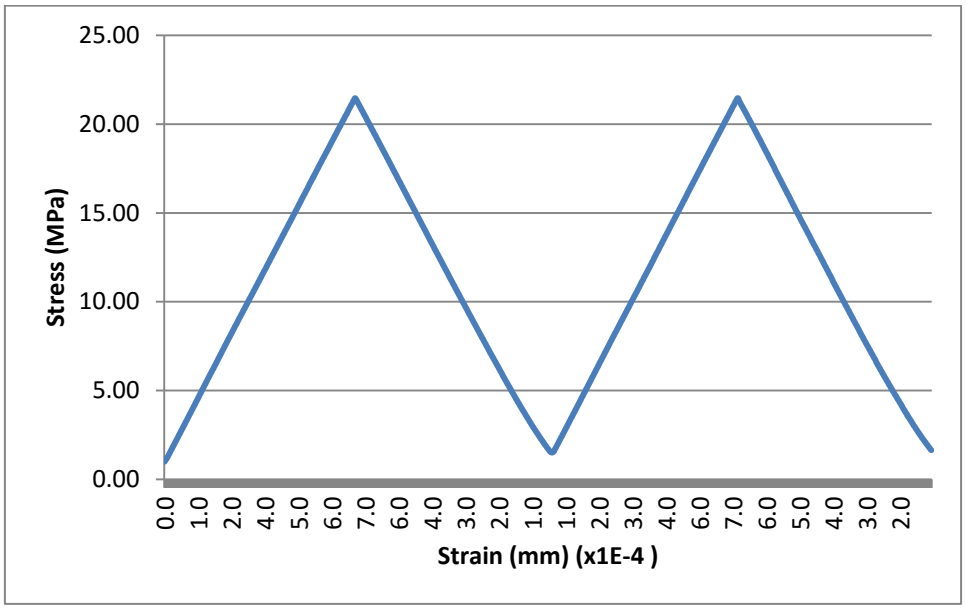

Figure 36: Stress-Strain graph of mix CM.

3.5 Modulus of Elasticity (MOE) Test Results

The values of the chord modulus of elasticity (MOE) of the testing cylinders of this study were calculated by the test machine from the experimental values of the stress and strain graphs as shown in Figure 36. The slope of the straight line in Figure

36 from 0.0001 to 0.0007 mm strain is the MOE of mix CM. The first graph is a trial one for calibration. The same procedure was used to find the MOE of all of the geopolymer concrete mixes. (Refer to Appendix A for the rest of stress-strain graphs). A summary of the MOE test results are shown in Figure 37.

Figure 37 shows that the modulus of elasticity of mix G100 is the highest among all the geopolymer concrete mixes with a value of 28.0 GPa, and also the closest to the control mix value. However, all the values of MOE for the geopolymer concrete mixes are less than the normal concrete mix (CM), which has a MOE value of 36 GPa.

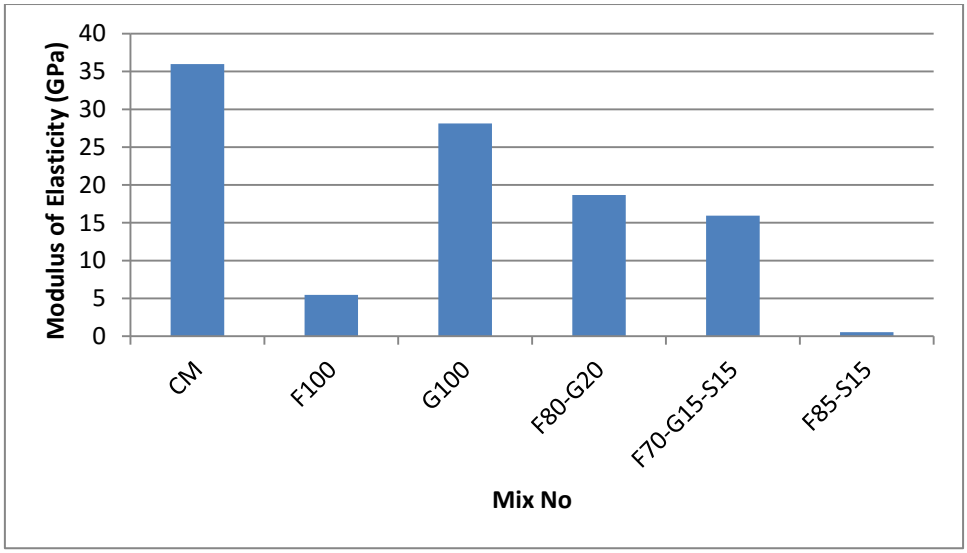

Figure 37: Modulus of elasticity test results of this study.

3.6 Rapid Chloride Penetration Test (RCPT) Results

The level of chloride penetration through the concrete specimen is a measure of its porosity and permeability. This test was conducted on all the concrete mixes of this study using test cylinders of diameter 100 mm and a thickness of 5 cm after 28 days of curing. A summary of the test results of this study are shown in Table 14 and Figure 38.

As Table 14 and Figure 38 show, the best geopolymer concrete mix in terms of permeability is also mix G100, which has moderate permeability class and is the closest to the control mix‘s low permeability. The highest permeability is for mix

F70-G15-S15; its permeability class was not specified due to over flow of chloride through the test sample. This means that the mix is extremely porous and has plenty of voids that allowed the chloride ions to penetrate through. Mix F100 with 100% fly ash also recorded a considerably high permeability level where the current overflowed through the sample. Addition of silica fume in mixes F70-G15-S15 and F85-S15 did not decrease their porosity as shown in Figure 38 where they showed over flow of chloride. This indicates that silica fume does not act as filler in the geopolymer concrete mixes.

Table 14: RCPT Results

Mix No	Charge (Coulombs)	Permeability Class
CM	1991	Low
F100	14407	Over Flow (perm. Class not specified)
G100	3847	Moderate
F80-G20	4233	Moderate
F70-G15-S15	14459	Over flow (perm. Class not specified)
F85-S15	11010	Over flow (perm. Class not specified)

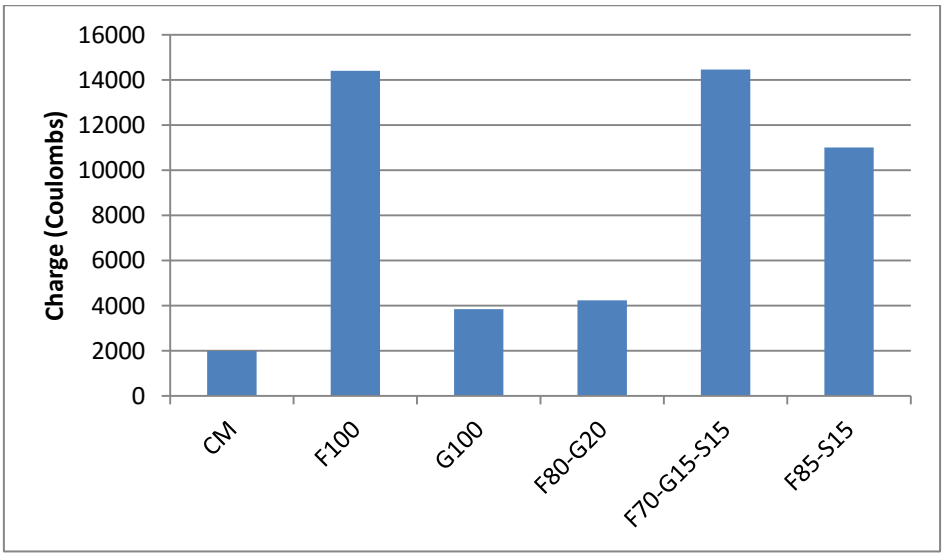

Figure 38: Rapid chloride penetration test results.

To assess the effect of oven curing on the permeability of geopolymer concrete, RCPT was conducted later on mixes G100 and F80-G20 extra samples that were oven cured. The results showed that oven curing is inefficient on decreasing the permeability of the geopolymer concrete specimens towards chloride ions. On the other hand, the electric charge (Coulombs) increased for the oven cured specimens compared with normal cured ones as Table 15 shows.

Table 15: RCPT results for oven cured specimens

Mix No.	G100	F80-G20
Charge (Coulombs)	10599	8508
Permeability Class	Over flow (perm. Class not specified)	Over flow (perm. Class not specified)

3.7 Microstructural Analysis Using SEM and EDS

Scanning electron microscopy (SEM) analyzes the microstructure of the test specimen. SEM test was first conducted on the normal concrete specimen (mix CM) after the specimen was prepared as described in Chapter 2. Backscattered mode was selected to show a clear image of the concrete specimens under high magnification factor. Figure 39 shows the SEM image of the control mix of this study at the age of 28 days, which has 100% OPC at a magnification factor of 2kx.

Figure 39 indicates the formation of C-S-H gel, which is the product of cement hydration, almost everywhere in the image. This implies that a complete reaction of normal concrete is achieved in the age of 28 days. Moreover, the morphology shows that mix CM has very few voids which was justified through having low permeability as it was shown earlier in Section 3.6. The same figure was analyzed using EDS for X-Ray analysis to investigate its chemical components. Figure 40 shows the spectrums selected for X-Ray analysis.

Figure 42 shows that spectrum 2 has a ratio of Ca to Si of 1.7 which falls in the range of 1.6 to 2, which is the range for Ca/Si ratio in the calcium silicate hydrate (C-S-H) gel of hydrated cement concrete specimens [32]. Figure 41 shows that Ca/Si is 6.5, which indicates that this is not a C-S-H gel and could be calcium hydroxide $Ca(OH)_2$ since also high amount of O_2 is present.

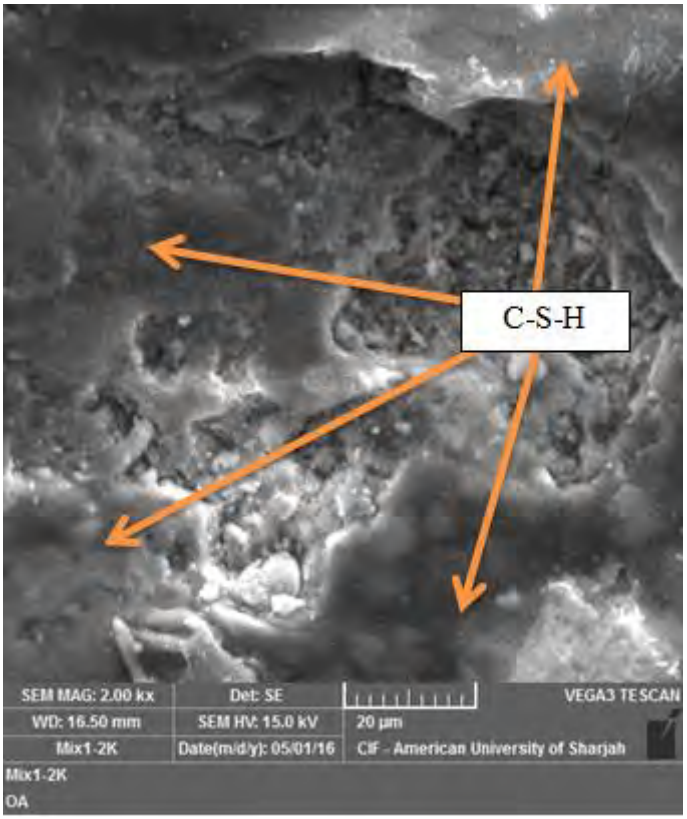

Figure 39: SEM image of mix CM at 28 days.

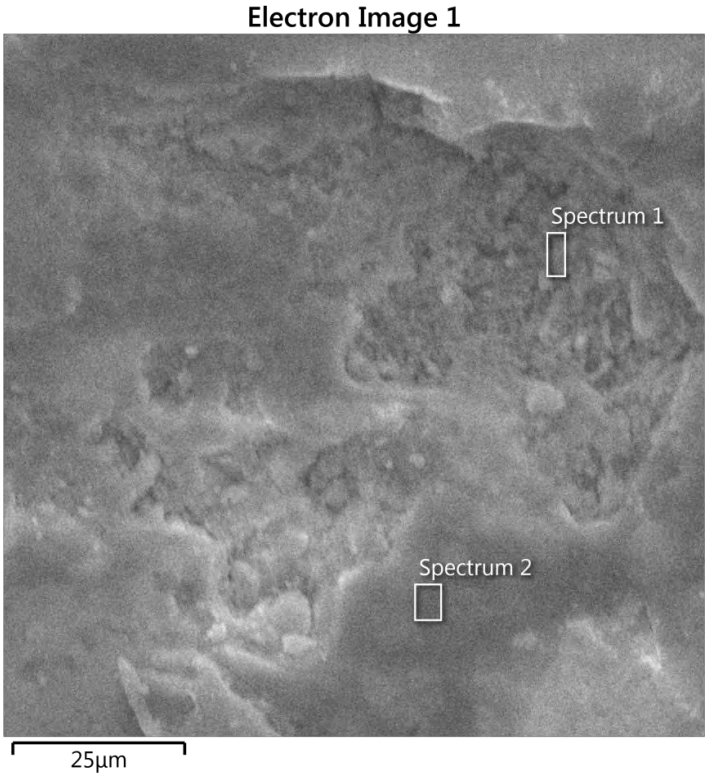

Figure 40: Spectrums of EDS analysis for mix CM.

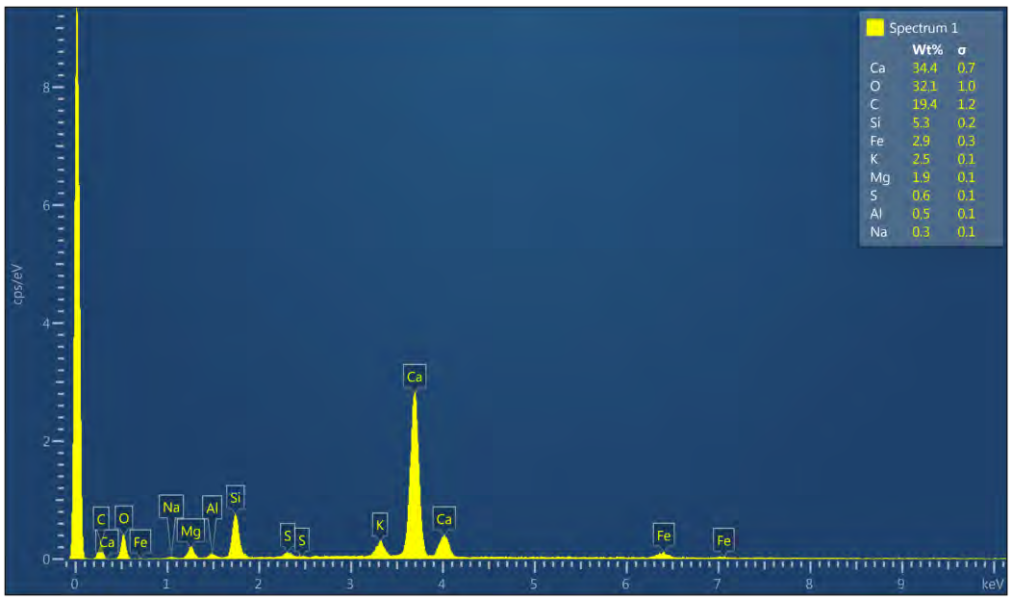

Figure 41: Chemical composition of spectrum 1 of mix CM.

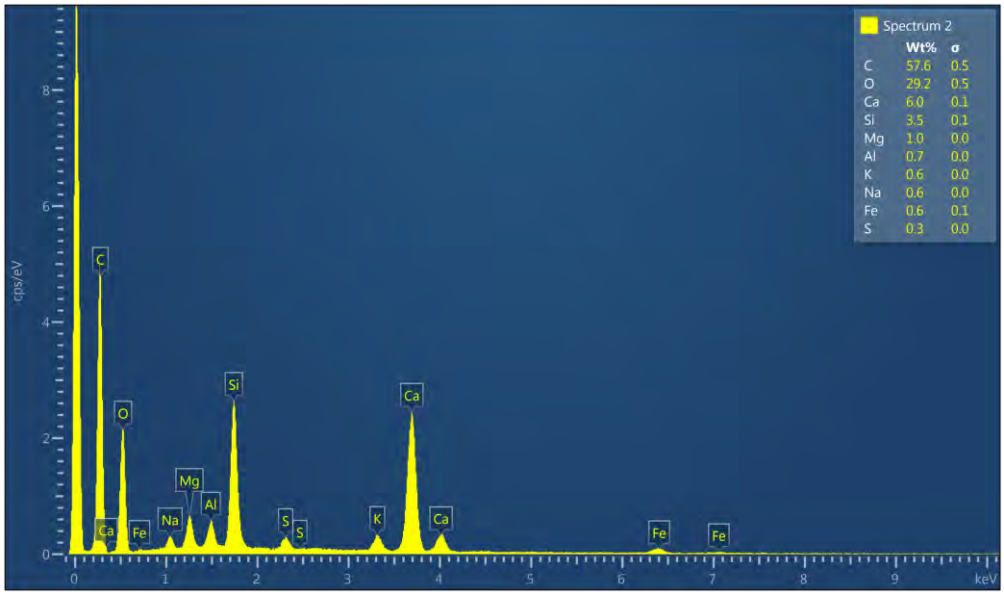

Figure 42: Chemical composition of spectrum 2 of mix CM.

The microstructure of mix F100 that is shown in Figure 43, with a magnification factor of 2k, indicates a deep void with several micro-cracks. This was clearly the cause of its very low strength obtained in Section 3.2 and very high permeability as shown earlier in Section 3.6.

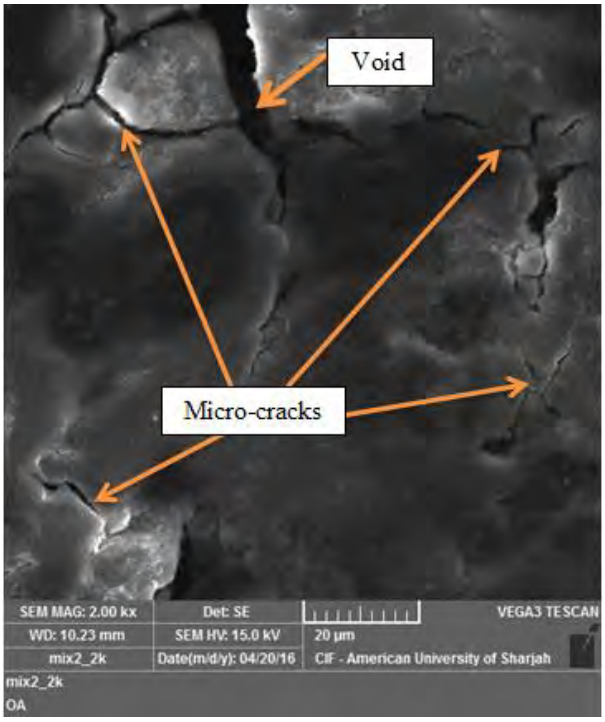

Figure 43: SEM image of mix F100 at 28 days.

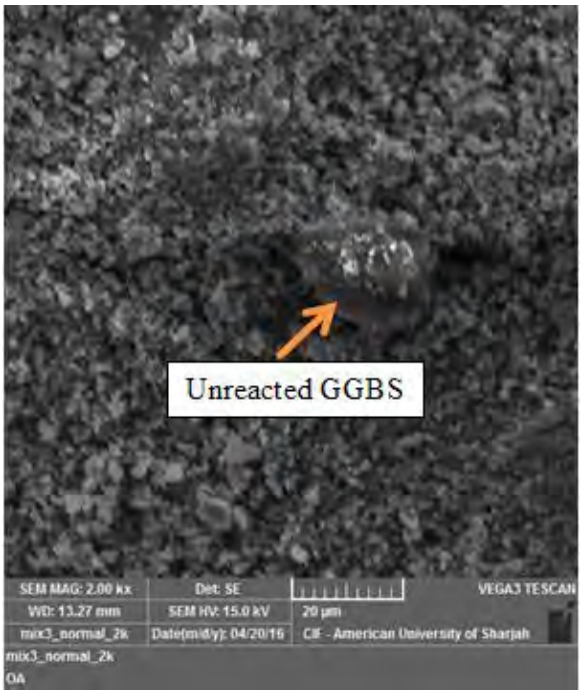

Figure 44: SEM image of ambient cured mix G100 specimen at 28 days.

Compared with Figure 43, mix G100 displayed in Figure 44 shows more amorphous microstructure than mix F100 specimen, yet more compactness and no cracks are detected for mix G100.

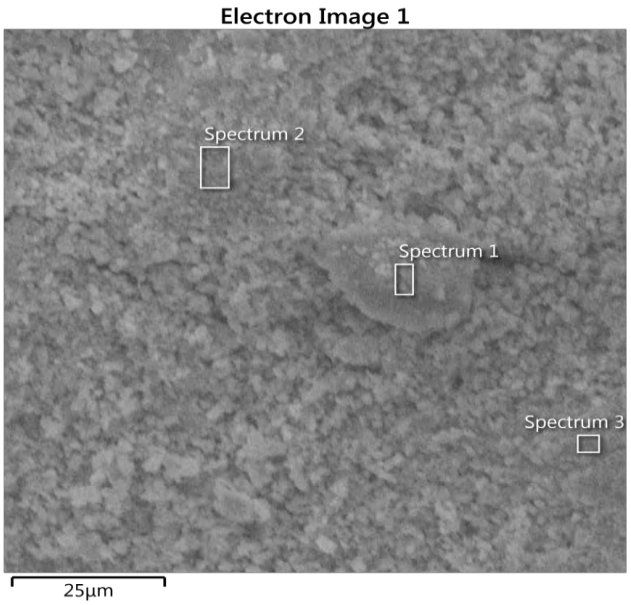

Figure 45: Spectrums for EDS analysis for mix G100.

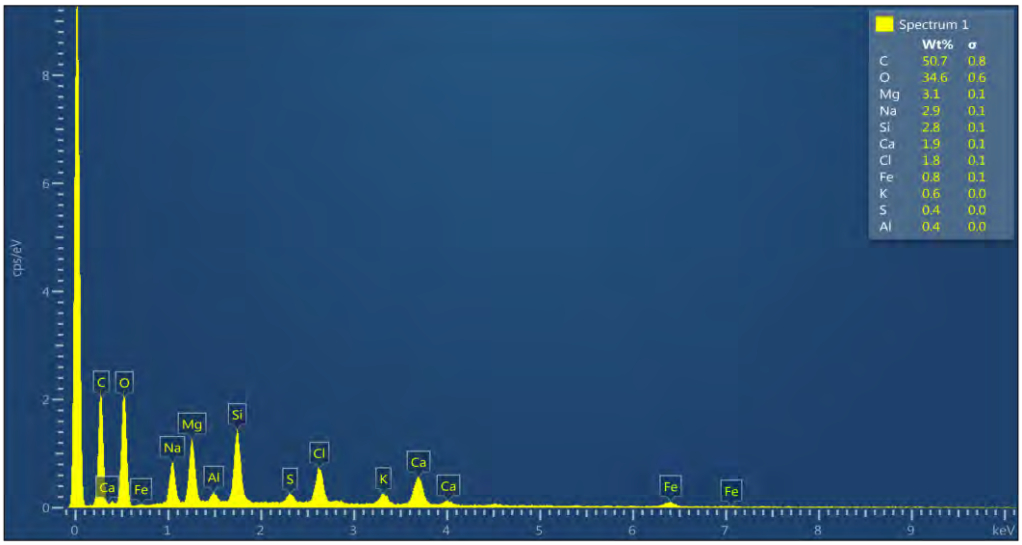

Figure 46: Chemical composition of spectrum 1 of ambient cured mix G100.

The EDS analysis of mix G100, shown in Figures 45-48, indicates that the reaction product presented by high ratio of Na/Al is in all the selected spectrums where the ratio ranged from 4.5 to 9.4. However, it was the lowest at spectrum 1, where high amount of calcite (carbon amount is 50.7 %) was detected. This shows that spectrum 1 indicates a partially reacted GGBS particle. High amount of calcite presented in GGBS particles could be the cause for the fast stiffening of concrete matrix during mixing process [6]. Geopolymer gel of calcium alumino-silicate (C-A-

S-H) can also be detected in high amounts through the ratio of Si/Al. For example, in spectrum 2, it is 9.4. The higher the Si/Al ratio is, the higher the compressive strength will be [15]. This was clear in mix G100 that recorded the highest compressive strength as shown earlier in section 3.2. The ratio of the Ca to Si was ranging from 0.26 to 0.68 in the three spectrums of Figure 45. This indicates some traces of C-S-H gel.

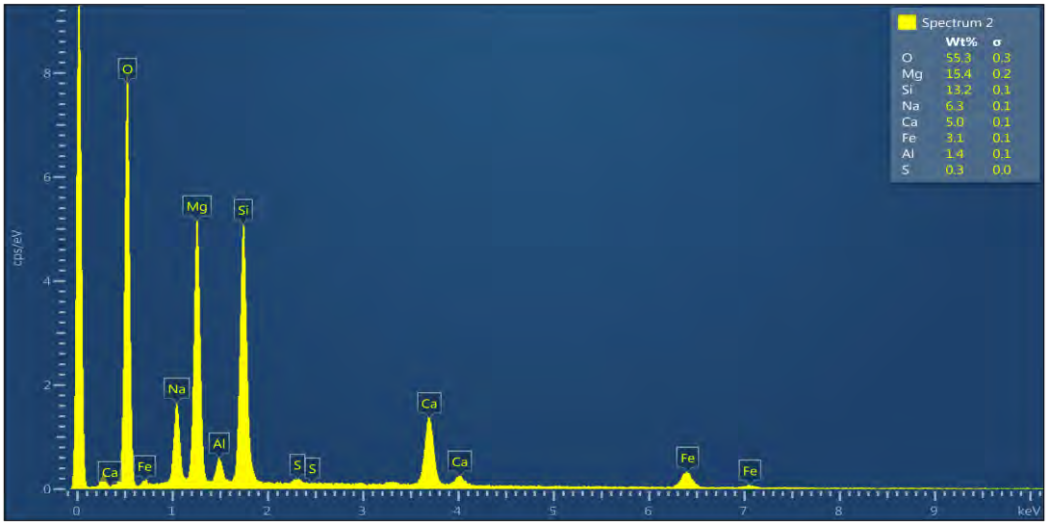

Figure 47: Chemical composition of spectrum 2 of ambient cured mix G100.

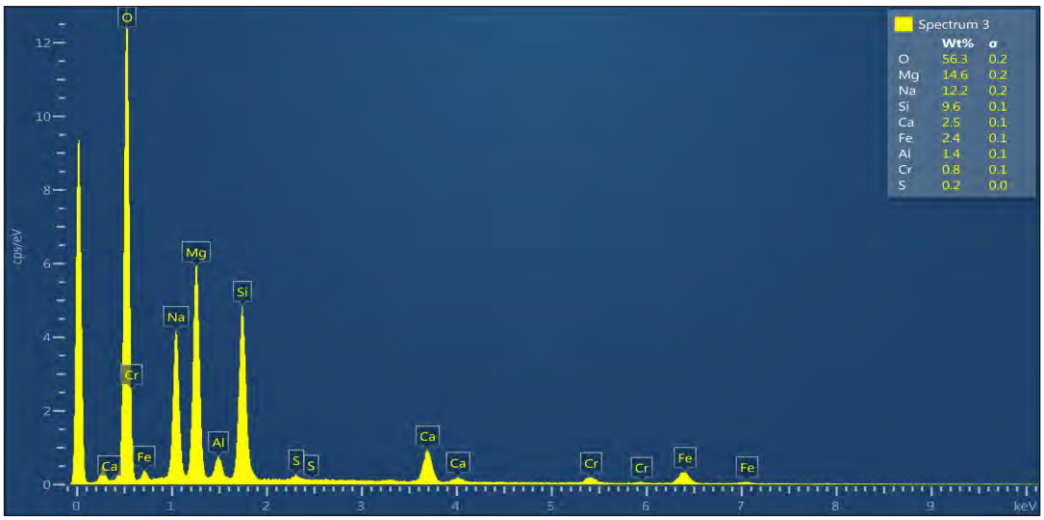

Figure 48: Chemical composition of spectrum 3 of ambient cured mix G100.

To compare the microstructures of the ambient cured and the oven cured specimens of mix G100, SEM image was taken for the oven cured specimen as shown in Figure 49. It is clear from the image that the mix has micro-cracks that were not

detected in the ambient cured sample shown in Figure 44. This explains the slightly less compressive strength obtained for oven cured sample of mix G100 as shown in Figure 28 in Section 3.2.

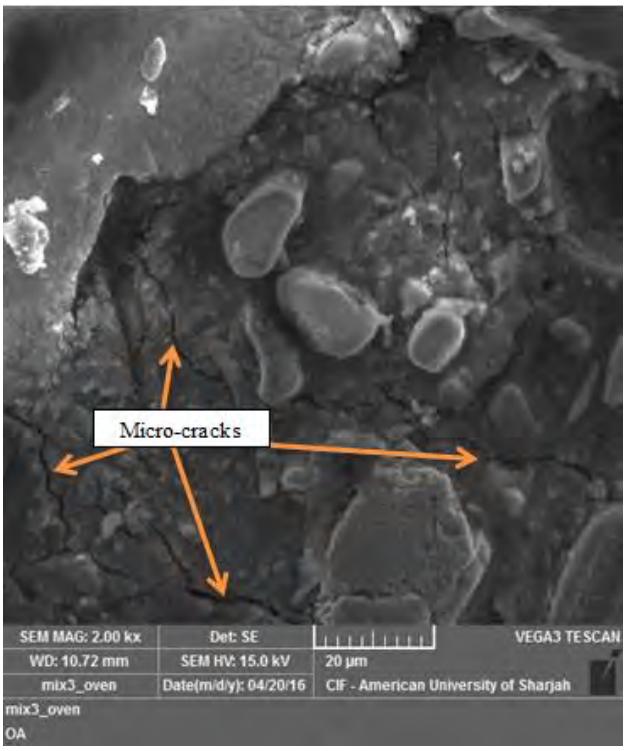

Figure 49: SEM image for oven cured G100 specimen.

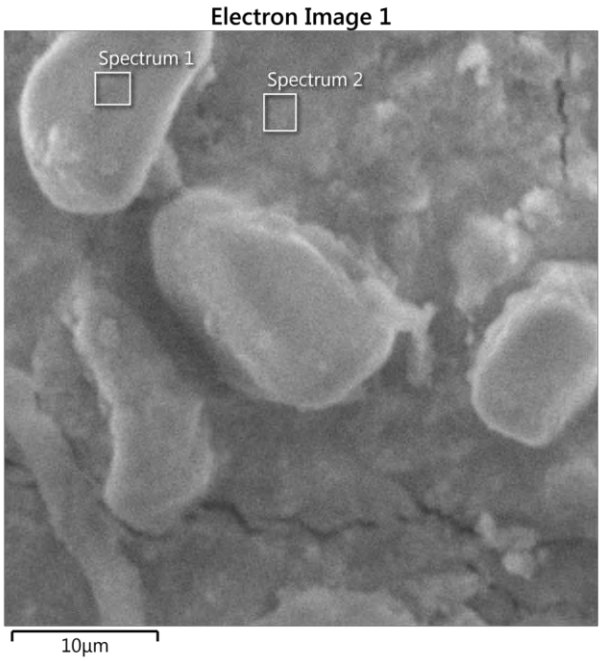

Figure 50: Spectrums for EDS analysis for oven cured specimen of mix G100.

Figure 49 was magnified and tested for EDS analysis as shown in Figure 50. The chemical composition shown in Figures 51 and 52 of the spectrums selected indicates low reaction product in spectrum 1 (Na/Al=0.5) and nothing in spectrum 2. Spectrum 1 indicates a calcite composition with high value of O and C. Moreover, a slight amount of alumino-silicate gel was detected. Oven cured specimen obtained lower ratios of Si/Al (2.1 in spectrum 1 and 3.6 in spectrum 2) than that of the ambient cured specimens which had a ratio of Si to Al up to 9.4. Therefore, it can be said that the oven curing was not beneficial in the case of 100% GGBS mix.

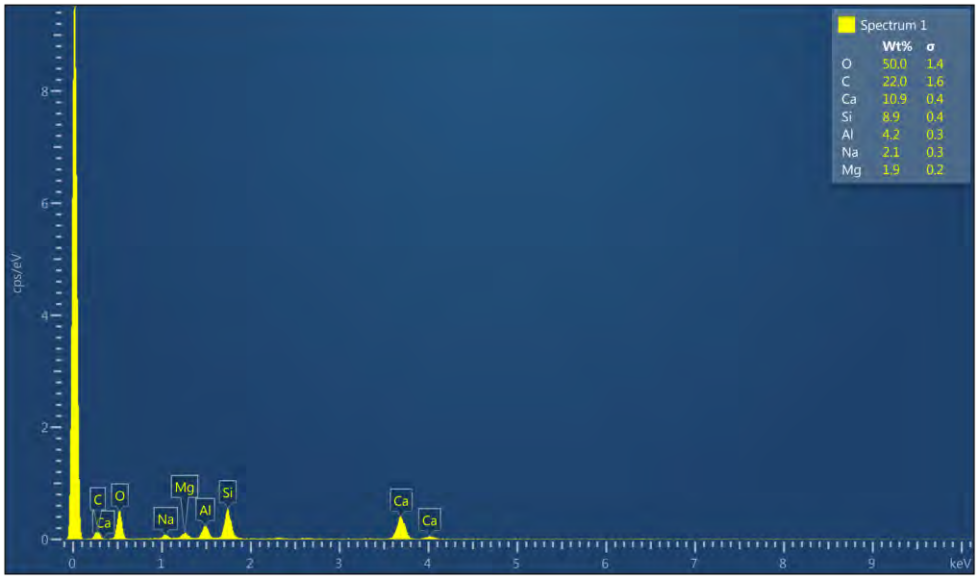

Figure 51: Chemical composition of spectrum 1 of oven cured mix G100.

Figure 52: Chemical composition of spectrum 2 of oven cured mix G100.

Figures 53a and 53b show very similar morphology for ambient cured specimens of mixes F70-G15-S15 and F85-S15. The chemical composition of the two specimens shows very small amounts of the reaction products compared to mix G100.

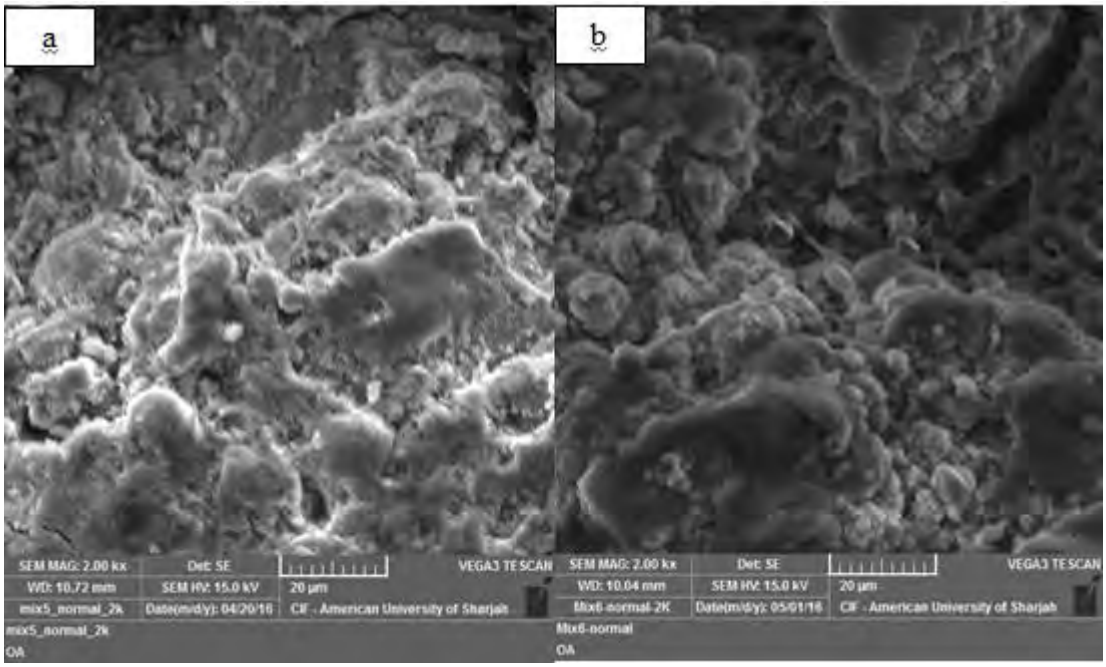

Figure 53: SEM images of mixes a) F70-G15-S15 and b) F85-S15 at ambient curing.

In general, chemical composition of the geopolymer concrete mixes of this study using EDS analysis showed that mix G100 recorded the highest ratio of Si/Al among all the geopolymer concrete mixes. This explains the highest compressive strength obtained for mix G100 among all other geopolymer concrete mixes of this study. Moreover, Ca/Si ratio was the highest as well. The high values of these two ratios show that high amounts of the two gels, (C-S-H) and (C-A-S-H), are present in mix G100.

Moreover, the comparison between the oven cured and the ambient cured specimens of mixes F80-G20, F70-G15-S15 and F85-S15 indicates that there are more reaction products in the oven cured specimens for these mixes. This was represented by higher ratios of Si/Al and Na/Al in the EDS analysis. Higher reaction products led to higher compressive strength when these specimens were oven cured as it was shown in Section 3.2. (Refer to Appendices B-G for more SEM and EDS images of this study.)

3.8 Evaluation of Carbon Emissions Results

The factors shown in Table 9 were used to calculate the carbon emissions arising from each of the mixes in this study as mentioned in Section 2.6.4. The procedure includes multiplying each ingredient quantity, used to prepare a concrete mix in this study, by its carbon factor and summing up the carbon emission of each ingredient to get the total of equivalent carbon emissions of the whole mix as an indicator of its carbon footprint. Table 16 shows the calculations for mix F100.

Table 16: Carbon dioxide emissions calculations for mix F100

Concrete Ingredient	Quantity (kg)	Carbon Dioxide Emissions (kg CO_2-e)
Coarse aggregate	61	0.3
Fine aggregate	47	0.66
Cement	0	0
Fly ash (F-type)	23	0.63
GGBS	0	0
Silica Fume	0	0
NaOH (pellets)	3.24	6.2
Concrete batching	142	0.47
	Total	8.26

The same procedure shown in Table 16 was used for all the concrete mixes of this study. Table 17 presents a summary of the final calculations of embodied equivalent carbon dioxide emissions of all mixes of this study and the percentage reduction compared to the emissions of the control mix (100% OPC).

Figure 54 shows that all the geopolymer concrete mixes have lower carbon dioxide emission potential than the normal concrete mix. Mix F85-S15 recorded the lowest carbon dioxide emissions and the highest percentage reduction with regard to the emissions of the control mix as shown in Table 17. This indicates that mix F85-S15, which contains 85% fly ash and 15% silica fume, is the ―greener‖ among all the mixes. Mix G100 with 100% GGBS had the highest carbon dioxide emissions among the geopolymer concrete mixes, yet still considerably lower than the emissions of the

control mix with OPC by almost half. This is due to the high fuel and electricity needed for producing, collecting, milling process, refining process, and transporting of steel alloys [5].

Table 17: Carbon dioxide emissions of all mixes of this study

Mix NO	Carbon Dioxide Emissions (kg CO_2-e)	% Reduction
CM	20.46	-
F100	8.26	59.63
G100	10.95	46.48
F80-G20	8.80	56.99
F70-G15-S15	8.62	57.87
F85-S15	8.22	59.82

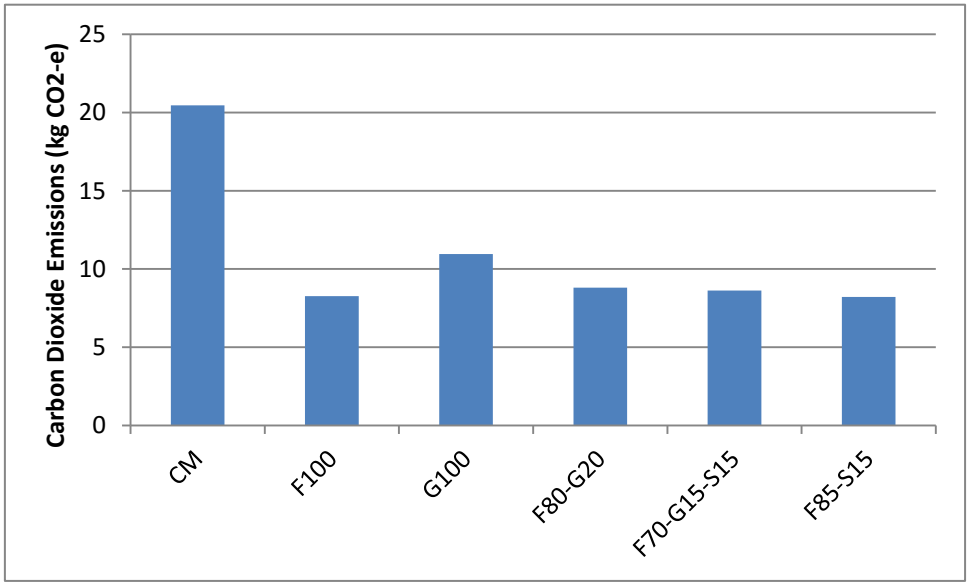

Figure 54: Comparison of CO_2 emissions of the mixes in this study.

3.9 Economic Feasibility Analysis Results

To calculate the cost of coarse aggregate, dune sand, crushed sand, and water in this study, the amount needed in each mix (as m^3 instead of kg) was calculated through dividing the quantity in kg by the bulk density (in kg/m^3) that was found earlier in this study and is presented in Table 4. Then, this amount was multiplied by

the cost per m^3 of material that is presented in Table 10. For example, the calculation of cost for coarse aggregate is as following:

Amount of coarse aggregate in m^3 = $\frac{1036.5\ \text{kg}}{1525\ kg/m3}$ = 0.68 m^3.

Cost of coarse aggregate per m^3 of concrete = 0.68 m^3 * 29.5 AED/m^3 = 20.0 AED/ m^3.

For the rest of materials, the quantities were converted from kg to ton, and then multiplied by the price/ton which is presented in Table 10. The cost of each concrete mix per cubic meter of concrete was found by summing up the costs of each of the concrete individual components. Table 18 shows the total cost of each concrete mix in this study.

Table 18: Cost Matrix (in AED) per m^3 of concrete for all mixes of this study

Material	CM	F100	G100	F80-G20	F70-G15-S15	F85-S15
Cement	86.24	0.0	0.0	0.0	0.0	0.0
Water	1.63	1.63	1.63	1.63	1.63	1.63
Fly ash	0.0	137.2	0.0	109.9	96.07	116.55
GGBS	0.0	0.0	86.24	17.27	12.98	0.0
Silica Fume	0.0	0.0	0.0	0.0	59	59
Coarse Aggregate	20.0	20.0	20.0	20.0	20.0	20.0
Dune Sand	4.26	4.26	4.26	4.26	4.26	4.26
Crushed Sand	8.98	8.98	8.98	8.98	8.98	8.98
NaOH (pellets)	0.0	296.3	296.3	296.3	296.3	296.3
Superplasticizer	3.75	3.75	3.75	3.75	3.75	3.75
Total cost/ m^3 of concrete	125	472	421	462	503	511

As Table 18 and Figure 55 show, geopolymer concretes have higher cost than normal concrete by almost 3 times. This high cost is due to the relatively expensive

NaOH pellets used to prepare the alkaline solution, which cost 5.4 AED per 1 kg. However, NaOH is a main contributor in the geopolymer concrete matrix prepared in this study, since it provides the needed alkaline environment that compensates the alkalinity of cement and allows for the dissolution of the silicon and aluminum ions from the reactive solids. Therefore, geopolymer binder cannot be formed without the presence of alkaline solution such as NaOH. Price of NaOH may decrease in the future with the growing of its demand and applications. As Table 18 shows, mix G100 is the cheapest among all the geopolymer concrete mixes prepared in this study.

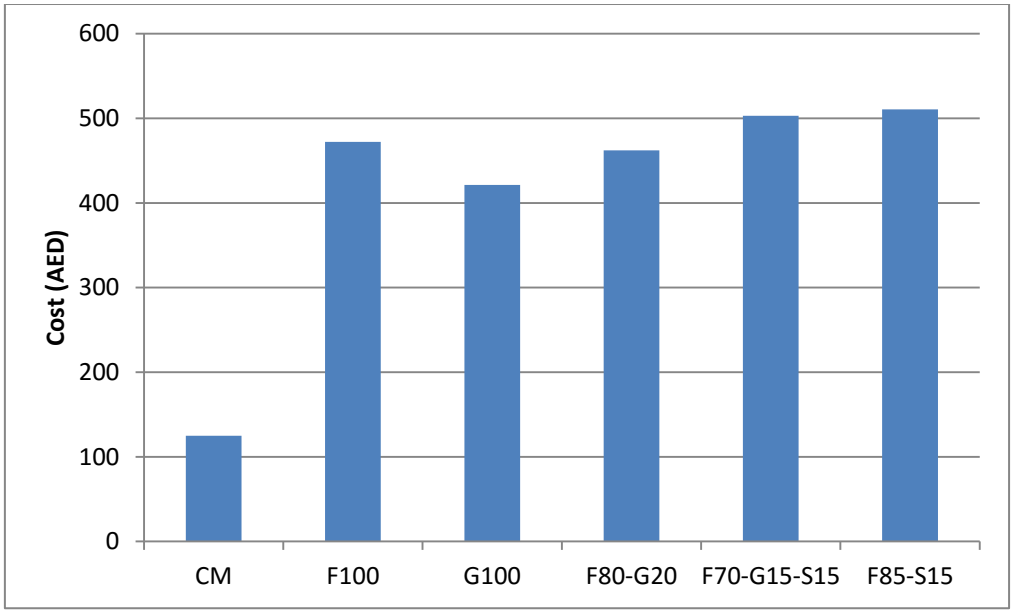

Figure 55: Cost of concrete mixes per cubic meter.

3.10 Summary of Results

Among all 6 geopolymer concrete mixes prepared in this study, G100 with 100% replacement of cement by GGBS can be considered as the best geopolymer mix due to its best performance in all the tests performed in this study. It recorded the highest compressive strength, flexural strength, elasticity modulus and tensile strength. In terms of durability, it also has the best performance with the least value of chloride penetration. This makes the concrete less susceptible to damage and cracks due to harsh environments, protects the steel from corrosion due to chloride penetration, and increases the life time of the structure. Its mechanical and durability performances were the most similar to the CM mix. The G100 mix has a tensile

strength that is even higher than the control mix. Ambient curing was found effective with mix G100 and can be considered for future use in site without the need for expensive heat curing. Good compactness and fewer cracks were detected through SEM images of the ambient cured specimen of this mix. Moreover, G100 mix recorded a considerable reduction of carbon emissions by releasing almost half the emissions of the control mix. However, cost feasibility analysis showed that geopolymer concrete is not economically feasible when compared to normal concrete.

Chapter 4: Conclusions and Future Studies

4.1 Conclusions

Different geopolymer concrete mixes were prepared for this study in the lab with different combinations of cement supplementary materials in an attempt to develop the best geopolymer mix in terms of mechanical performance, durability, and carbon footprint that can replace the use of cement completely in concrete production for structural use. The following points summarize the investigations carried out in this study and the findings:

- Six geopolymer concrete mixes were developed and tested in the laboratory using different combinations of cement supplementary materials, class F-fly ash, GGBS, and silica fume, to replace cement completely in the concrete matrix. A mix with the best performance was suggested.
- Slump and air content tests were performed on fresh concrete mixes and showed extremely stiff geopolymer concrete behavior for all the geopolymer mixes with very low workability and sometimes no slump and a high air content. Superplasticizer was not considerably beneficial in improving the workability due to the high viscous nature of the geopolymer paste.
- A compressive strength test was conducted on all mixes at 7 and 28 days of curing. It was also conducted on ambient cured and oven cured samples at 28 days. Results showed that very low compressive strength was obtained by the geopolymer concrete mixes in comparison to the normal concrete mix with 100% OPC, except for mix G100 that has 100% GGBS replacement of OPC. G100 mix recorded a 28 MPa compressive strength in 7 days and 36 MPa in 28 days without the need for heat curing. Other mixes showed significant increase in 28-days compressive strength when subjected to heat curing; up to 99% increase was obtained in mix F85-S15. Failure plane propagated through the geopolymer concrete binder in the age

of 7 days while it went through both the aggregate and binder at the at the age of 28 days, allowing the aggregate to carry load at the late age.

- The tensile strength test showed best performance of mix G100 among all mixes, even better than the control mix, with tensile strength of 2.8 MPa in 28 days.
- The flexural strength test also showed best performance of G100 mix over the rest of the geopolymer concrete mixes.
- The modulus of Elasticity (MOE) test was the best when also 100% GGBS was used (mix G100).
- A rapid Chloride Penetration Test (RCPT) was conducted on the concrete samples to investigate the concrete durability against chloride penetration. Mix G100 recorded the best performance in durability with moderate permeability class; whereas, most of the other geopolymer concrete mixes had over flow of chloride ions.
- Scanning Electron Microscopy (SEM) and Energy Dispersive Spectroscopy (EDS) analyses were conducted on the concrete samples of this study in order to investigate its microstructure and chemical composition. Mix G100 recorded a smaller number of micro-cracks and higher amounts of reaction gels of (C-H) and (C-S-H) than the other geopolymer concrete mixes, which explains its better performance in terms of mechanical properties and durability.
- A carbon footprint evaluation was carried out in this study by calculating the carbon emissions arising from the production of each of the concrete mixes developed in this study. Results showed lower carbon emissions of all the geopolymer concrete mixes compared with the control mix that has considerably high carbon emissions due to cement that contributes to most of the production process of concrete and has a very high carbon emissions factor. Therefore, geopolymer concrete is effective to have a more sustainable and green construction if implemented in the structural uses. Based on the results of this study, geopolymer concrete has the potential to cut down CO_2 emissions of concrete production for up to 60%.

- Addition of silica fume was ineffective to produce geopolymer concrete, which was clear in the mixes containing silica fume that did not perform efficiently in the tests conducted in this study.
- Geopolymer concrete with 100% replacement of cement by GGBS can perform in a considerably similar way to normal concrete in terms of mechanical behavior and durability against chloride.
- A cost analysis study was conducted by calculating the cost of preparing 1 m^3 of each of the concrete mixes in this study. The costs of individual components used to prepare 1 m^3 of the concrete mix were summed up. Economic feasibility study showed that geopolymer concrete has relatively higher cost than normal concrete due to the high cost of alkaline solution used in the geopolymer concrete.

4.2 Future Studies

Based on the above conclusions, it is recommended for future studies to consider the replacement of cement totally by GGBS with some improvement in the mix for a better strength and workability.

To improve the workability of the geopolymer concrete, it is recommended for future studies to increase the amount of alkaline solution in the mix to an extent that does not affect the strength.

Future studies may also use higher concentration of NaOH solution to improve the geopolymer concrete strength, or a combination with another alkaline solution that is rich in silicate, such as sodium silicate solution.

In order to reduce the geopolymer concrete cost, future investigations may try to find out methods of producing NaOH at lower cost that can make geopolymer concrete more economically feasible when compared to normal concrete.

Geopolymer concrete is becoming more promising in terms of waste reuse, carbon footprint, and renewable resources availability.

References

[1] Z. Zhang, J. L. Provis, A. Reid, and H. Wang, "Geopolymer foam concrete: An emerging material for sustainable construction," *Construction and Building Materials*, vol. 56, pp. 113–127, Apr. 2014.

[2] F. Aslani, "Thermal Performance Modeling of Geopolymer Concrete," *Journal of Materials in Civil Engineering,* vol. 28, Jan. 2016.

[3] M. Elchalakani, T. Aly, and E. Abu-Aisheh, "Sustainable concrete with high volume GGBFS to build Masdar city in the UAE," *Case Studies in Construction Materials*, vol. 1, pp. 10–24, 2014.

[4] T. Proske, S. Hainer, M. Rezvani, and C.-A. Graubner, "Eco-friendly concretes with reduced water and cement contents — mix design principles and laboratory tests," *Cement and Concrete Research*, vol. 51, pp. 38–46, Sep. 2013.

[5] D. J. M. Flower and J. G. Sanjayan, "Green house gas emissions due to concrete manufacture,"*The International Journal of Life Cycle Assessment*, vol. 12, no. 5, pp. 282–288, May 2007.

[6] D. Ravikumar, S. Peethamparan, and N. Neithalath, "Structure and strength of NaOH activated concretes containing fly ash or GGBFS as the sole binder," *Cement and Concrete Composites*, vol. 32, no. 6, pp. 399–410, Jul. 2010.

[7] F. N. Okoye, J. Durgaprasad, and N. B. Singh, "Effect of silica fume on the mechanical properties of fly ash based-geopolymer concrete," *Ceramics International*, vol. 42, no. 2, pp. 3000–3006, Feb. 2016.

[8] P. Van den Heede and N. De Belie, "Environmental impact and life cycle assessment (LCA) of traditional and ‗green' concretes: Literature review and theoretical calculations," *Cement and Concrete Composites*, vol. 34, no. 4, pp. 431–442, Apr. 2012.

[9] A. Motorwala, V. Shah, R. Kammula, P. Nannapaneni, and D.B. Raijiwala, "ALKALI Activated FLY-ASH Based Geopolymer Concrete," *International Journal of Emerging Technology and Advanced Engineering*, vol. 3, no. 1, pp. 2250-2459, 2013.

[10] D. L. Y. Kong and J. G. Sanjayan, "Effect of elevated temperatures on geopolymer paste, mortar and concrete," *Cement and Concrete Research*, vol. 40, no. 2, pp. 334–339, Feb. 2010.

[11] B. A. Latella, D. S. Perera, D. Durce, E. G. Mehrtens, and J. Davis, "Mechanical properties of metakaolin-based geopolymers with molar ratios of Si/al ≈ 2 and na/al ≈ 1," *Journal of Materials Science*, vol. 43, no. 8, pp. 2693–2699, Feb. 2008.

[12] E. I. Diaz-Loya, E. N. Allouche, and S. Vaidya, "Mechanical Properties of Fly-Ash-Based Geopolymer Concrete," *ACI Materials Journal,* vol. 108, pp. 300-306, 2011.

[13] M. I. Abdul Aleem, and P. D. Arumairaj, "Optimum mix for the geopolymer concrete, " *Indian Journal of Science and Technology*, vol. 5, no. 3, pp. 2299-2301, 2012.

[14] P. Duxson and J. L. Provis, "Designing precursors for Geopolymer Cements," *Journal of the American Ceramic Society*, vol. 91, no. 12, pp. 3864–3869, Dec. 2008.

[15] P. Nath and P. K. Sarker, "Effect of GGBFS on setting, workability and early strength properties of fly ash geopolymer concrete cured in ambient condition," *Construction and Building Materials*, vol. 66, pp. 163–171, Sep. 2014.

[16] S. A. Khedr, and M. N. Abou-Zeid, "Characteristics of Silica-Fume concrete," *Journal of Materials in Civil Engineering*, vol. 6, no. 3, pp. 357-375, 1994.

[17] M. A. A. Abd Elaty and M. F. Ghazy, "Performance of Portland cement mixes containing silica fume and mixed with lime-water," *HBRC Journal*, vol. 10, no. 3, pp. 247–257, Dec. 2014.

[18] N. K. Lee, G. H. An, K. T. Koh, and G. S. Ryu, "Improved reactivity of fly ash-slag Geopolymer by the addition of silica Fume," *Advances in Materials Science and Engineering*, vol. 2016, pp. 1–11, 2016.

[19] T. Bakharev, "Resistance of geopolymer materials to acid attack," *Cement and Concrete Research*, vol. 35, no. 4, pp. 658–670, Apr. 2005.

[20] A. Hajimohammadi, J. L. Provis, and J. S. J. van Deventer, "The effect of silica availability on the mechanism of geopolymerisation," *Cement and Concrete Research*, vol. 41, no. 3, pp. 210–216, Mar. 2011.

[21] J. Temuujin, A. van Riessen, and K. J. D. MacKenzie, "Preparation and characterisation of fly ash based geopolymer mortars," *Construction and Building Materials*, vol. 24, no. 10, pp. 1906–1910, Oct. 2010.

[22] G. S. Ryu, Y. B. Lee, K. T. Koh, and Y. S. Chung, "The mechanical properties of fly ash-based geopolymer concrete with alkaline activators," *Construction and Building Materials*, vol. 47, pp. 409–418, Oct. 2013.

[23] D. Bondar, "Geo-polymer concrete as a new type of sustainable construction materials, " in:Proceedings of the Third International Conference on Sustainable Construction Materials and Technologies, Available: http://www.claisse. info/Proceeding.htm. Accessed: April 20, 2016.

[24] P.-C. Aitcin and B. B. Stern, *High-performance concrete* vol. 5; New York; London;: E & FN Spon, 1998.

[25] P. Joshi and C. Chan, "Rapid chloride permeability testing," *Concrete Construction,* vol. 47, pp. 37-43, 2002.

[26] R. F. Egerton and R. Egerton, *Physical principles of electron microscopy: An introduction to TEM, SEM, and AEM*. New York: Springer Science+Business Media, 2008.

[27] S. Vares and T. Ha¨kkinen, "Environmental burdens of concrete and concrete products," *Nordic Concrete Research*, 21, 1/98, 1998, Available: http://www.betong.net/ikbViewer/Content/739021/doc-21-10.pdf, Accessed: May 5, 2016.

[28] G. Hammond, C. Jones, F. Lowrie, P. Tse, M. G. Hammond, and C. Jones, *Embodied carbon: The inventory of carbon and energy (ICE)*, F. Lowrie, Ed., 5th ed. Bracknell: BSRIA, 2011.

[29] P. Wu and S. P. Low, *Lean and cleaner production: Applications in Prefabrication to reduce carbon emissions*. Berlin: Springer-Verlag Berlin and Heidelberg GmbH & Co. K, 2013.

[30] L. K. Turner and F. G. Collins, "Carbon dioxide equivalent (CO2-e) emissions: A comparison between geopolymer and OPC cement concrete," *Construction and Building Materials*, vol. 43, pp. 125–130, Jun. 2013.

[31] Norchem, "Silica Fume applications in sustainability,". [Online]. Available: http://www.norchem.com/applications-sustainability.html. Accessed: May 5, 2016.

[32] W. Kurdowski and SpringerLink, *Cement and Concrete Chemistry*. Dordrecht: Springer Netherlands, 2014.

Appendix A: Stress-train Graphs for Geopolymer Concrete Mixes of This Study

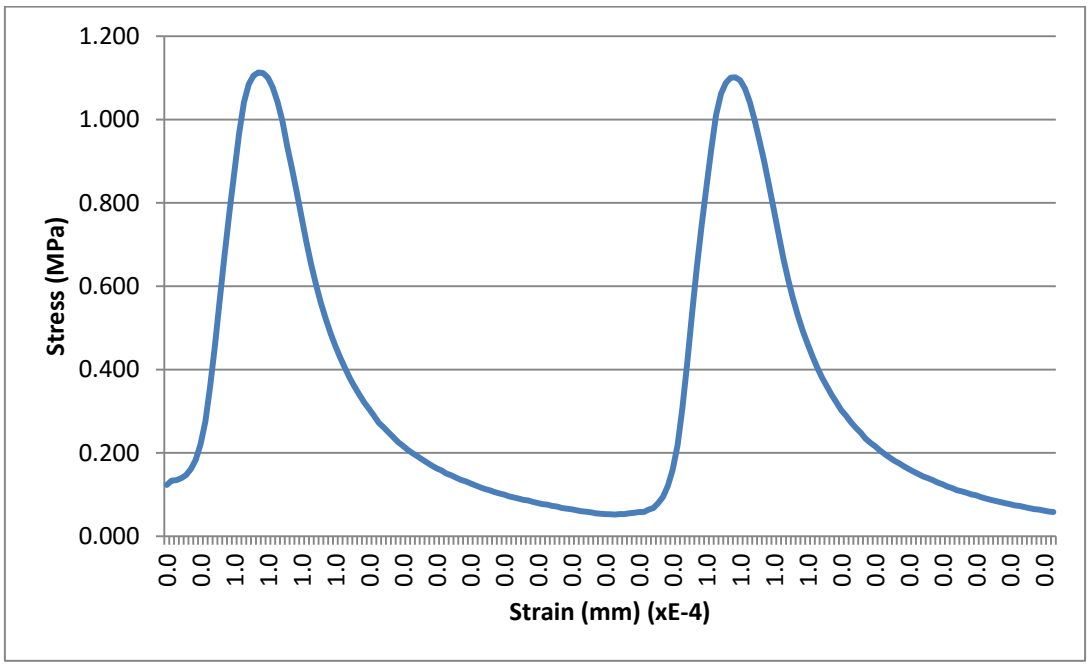

Figure A 1: Stress-strain graph for mix F100.

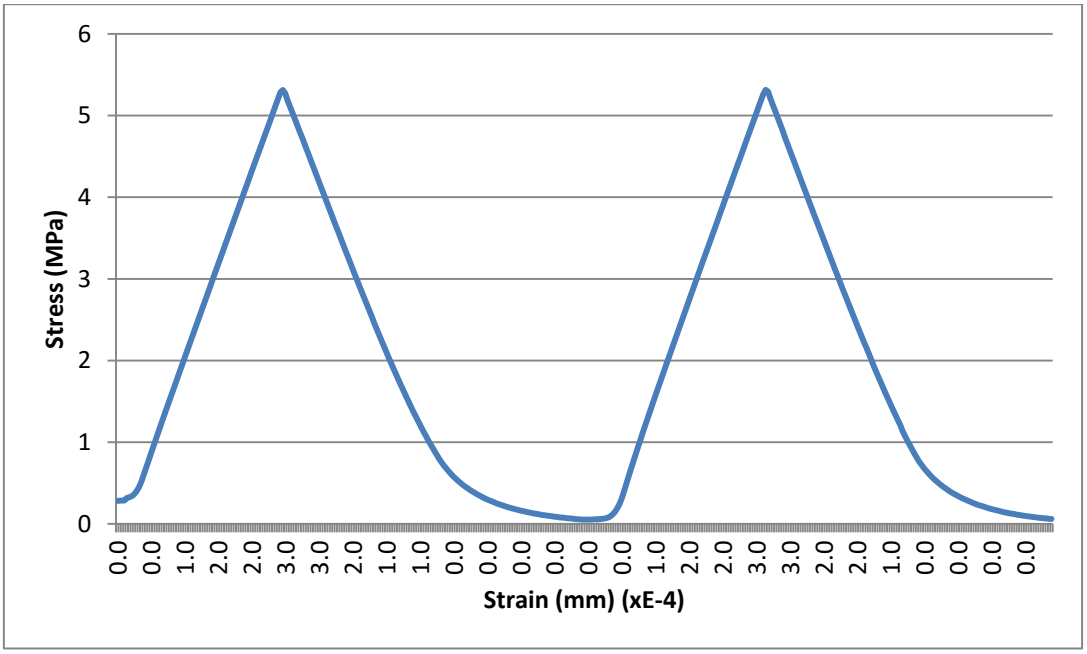

Figure A 2: Stress-strain graph for mix F80-G20.

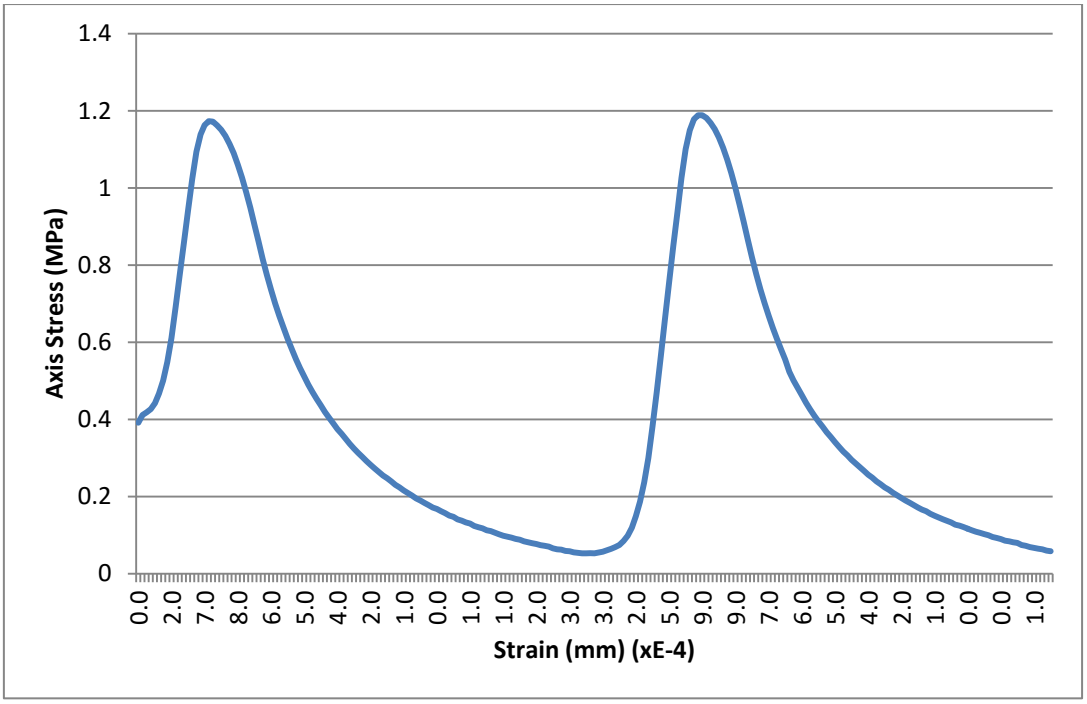

Figure A 3: Stress-strain graph for mix F70-G15-S15.

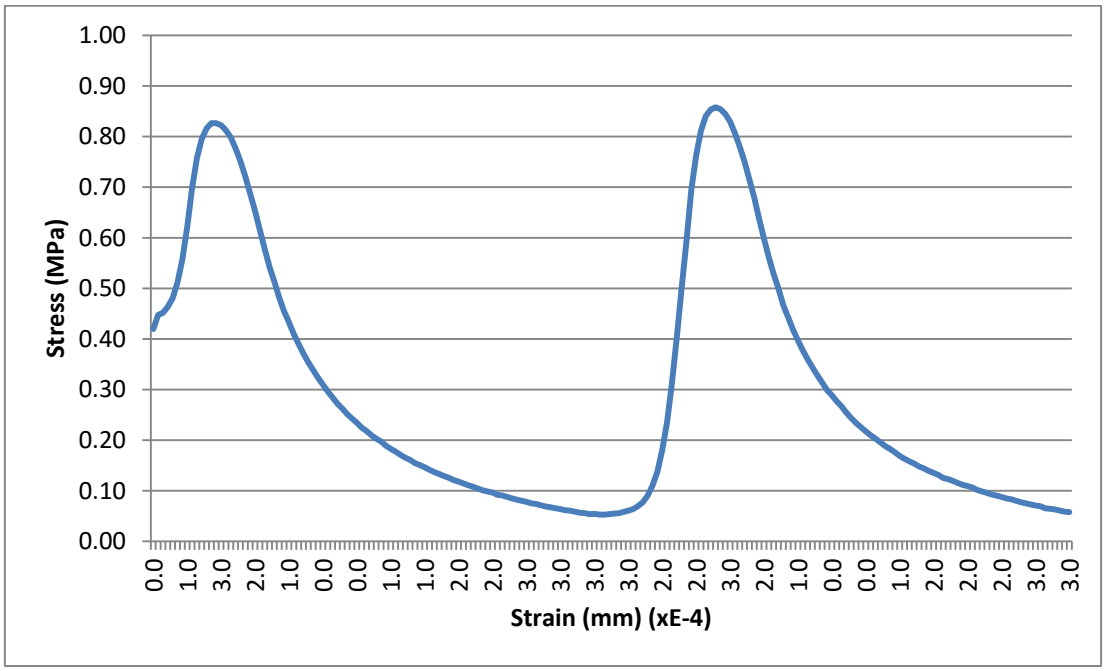

Figure A 4: Stress-strain graph for mix F85-S15.

Appendix B: SEM and EDS for ambient cured specimen of mix F80-G20

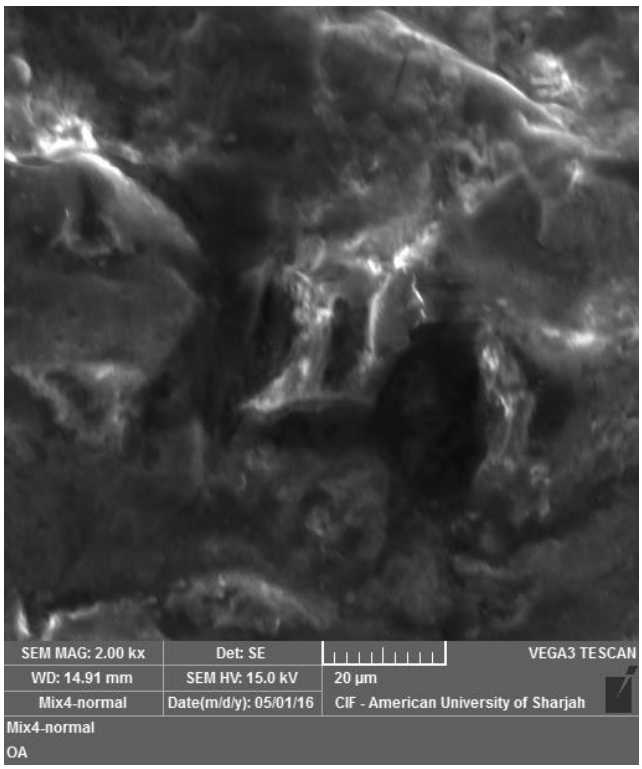

Figure B 1: Ambient cured specimen of mix F80-G20 under SEM.

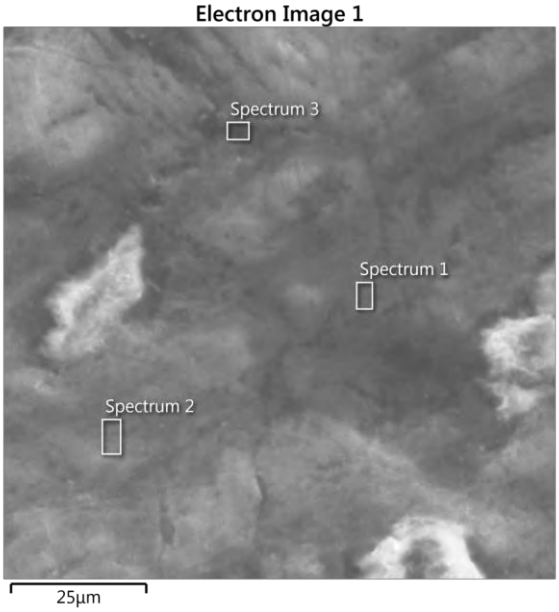

Figure B 2: Selected spectrums of the image of ambient cured specimen of mix F80-G20 under EDS analysis.

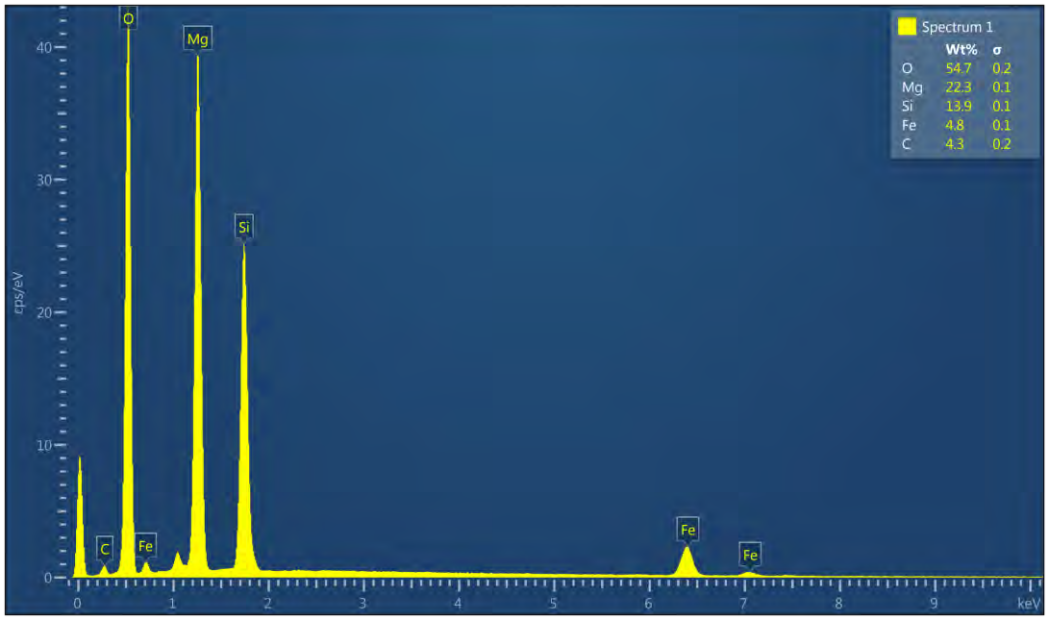

Figure B 3: Chemical composition at spectrum 1 of mix F80-G20.

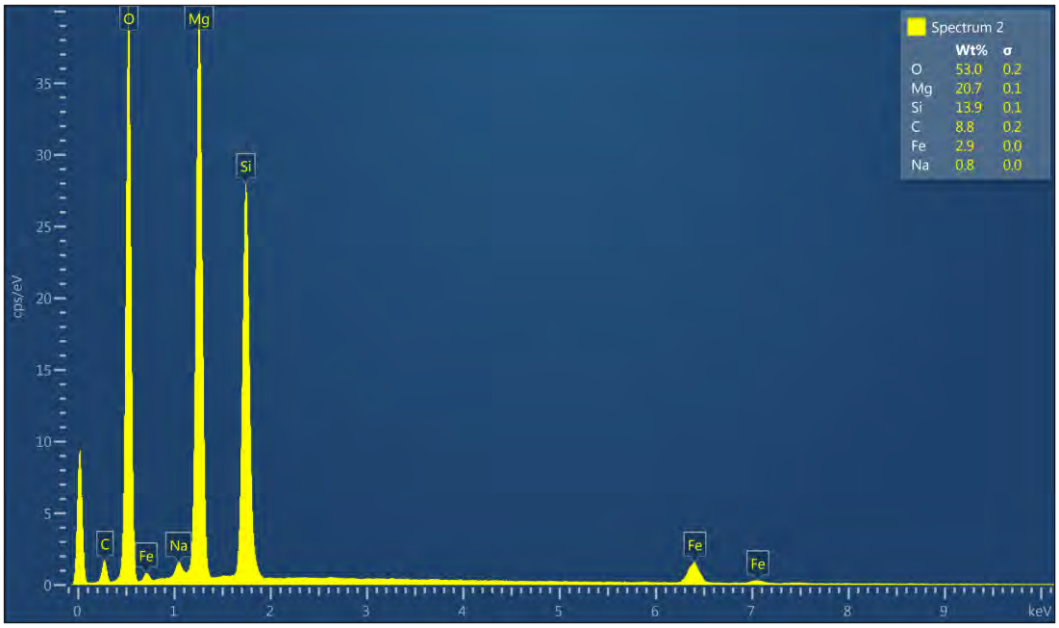

Figure B 4: Chemical composition at spectrum 2 of mix F80-G20.

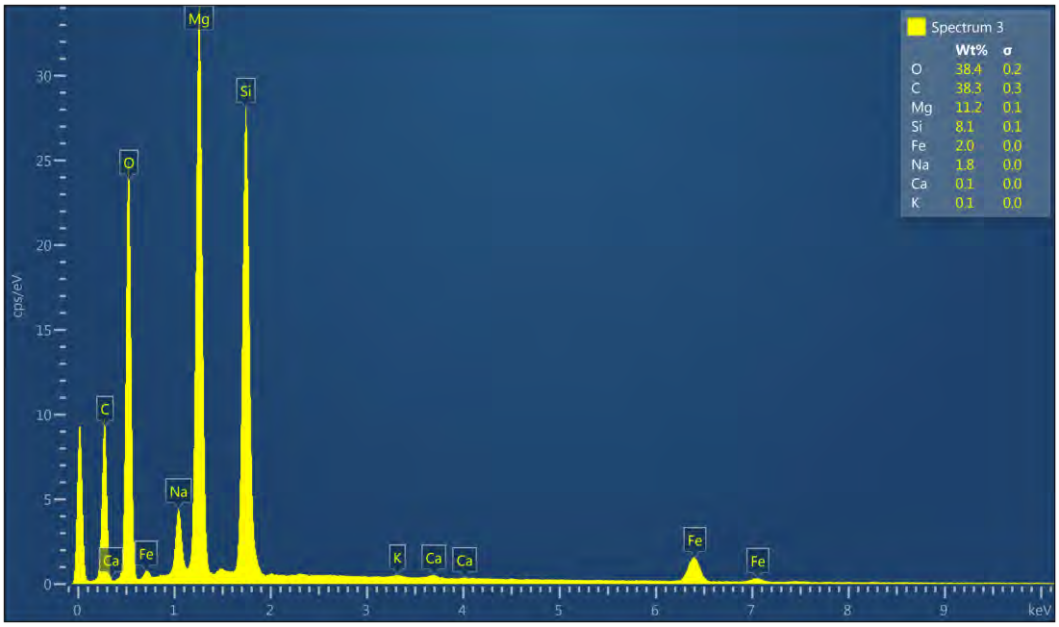

Figure B 5: Chemical composition at spectrum 3 of mix F80-G20.

Appendix C: SEM and EDS for oven cured specimen of mix F80-G20

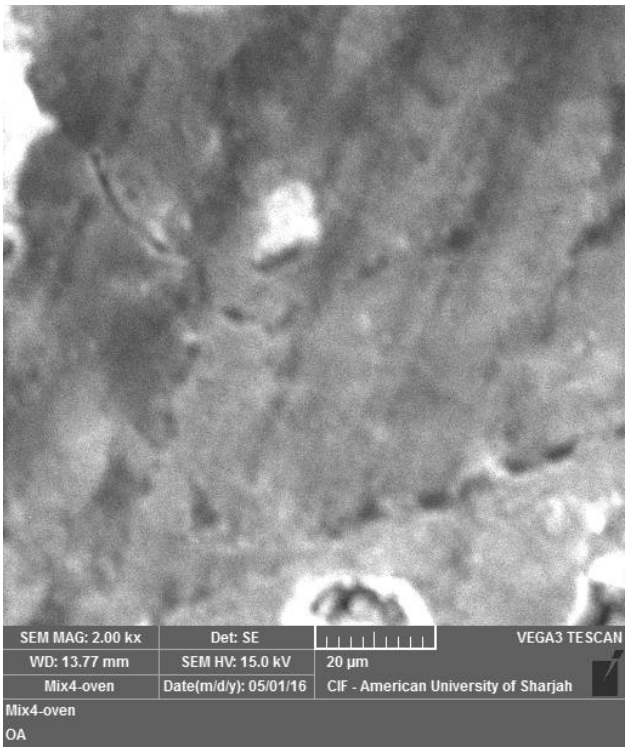

Figure C 1: Oven cured specimen of mix F80-G20 under SEM.

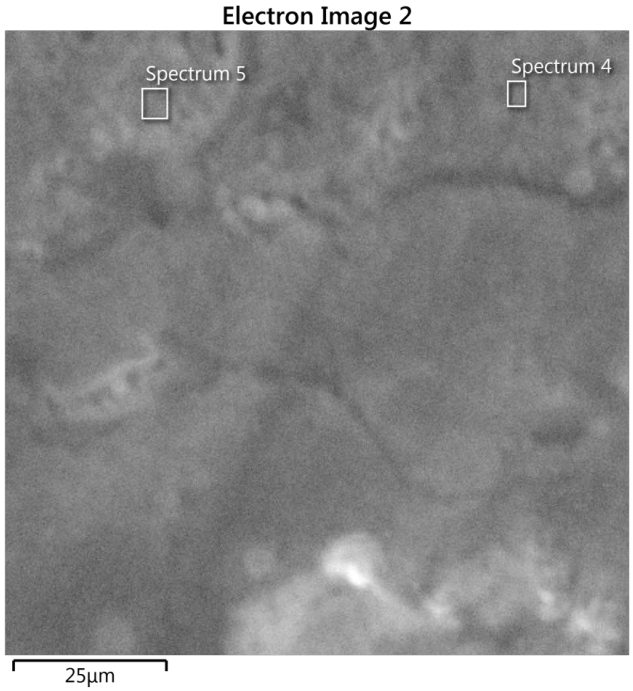

Figure C 2: Selected spectrums of the image of oven cured specimen of mix F80-G20 under EDS analysis.

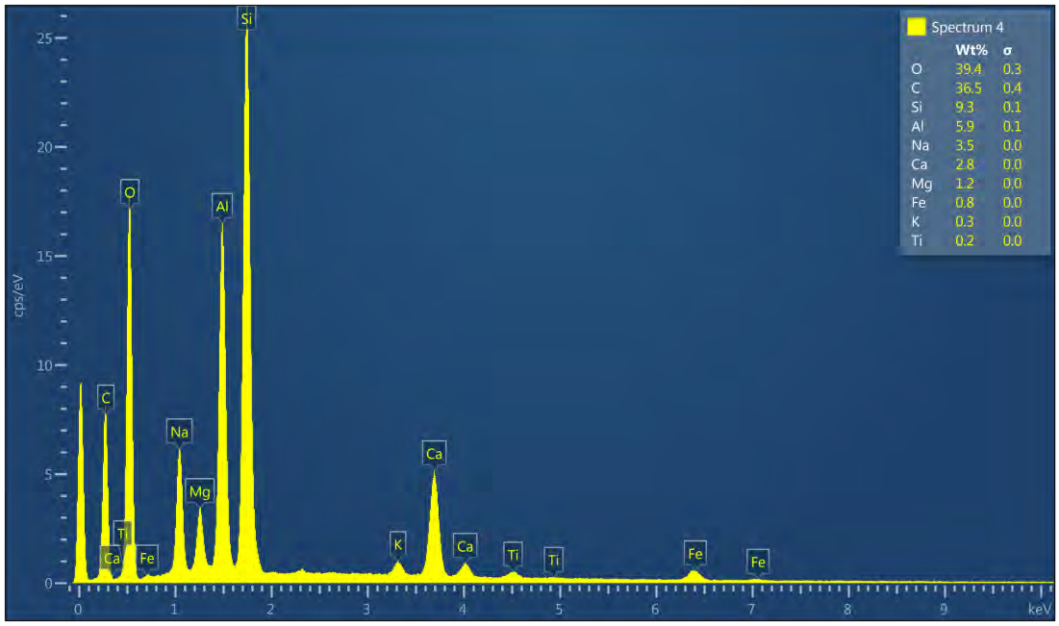

Figure C 3: Chemical composition at spectrum 4 of mix F80-G20.

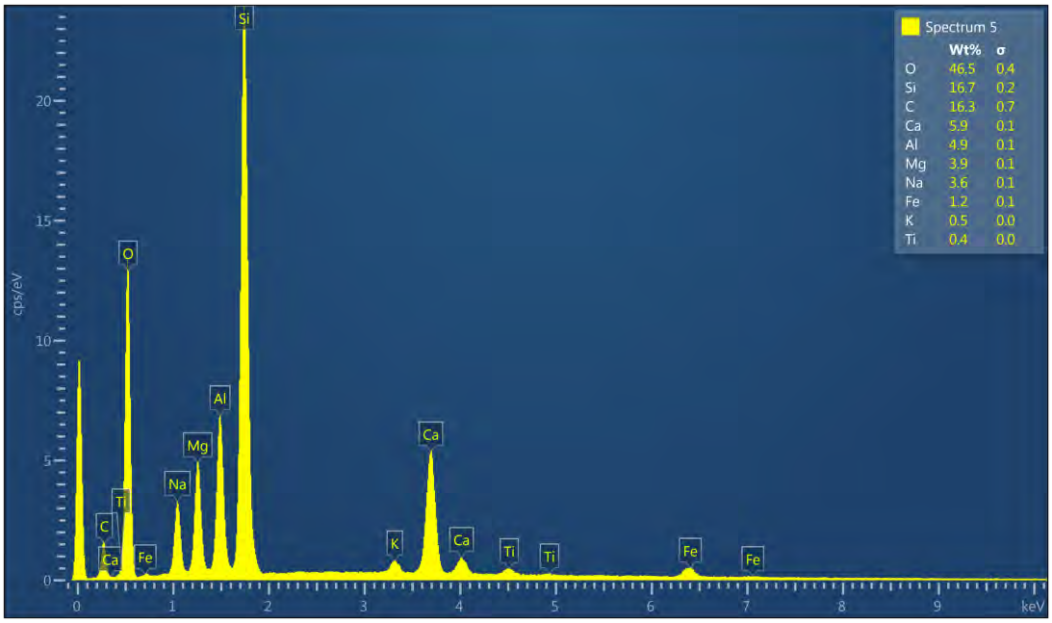

Figure C 4: Chemical composition at spectrum 5 of mix F80-G20.

Appendix D: EDS for ambient cured specimen of mix F70-G15-S15

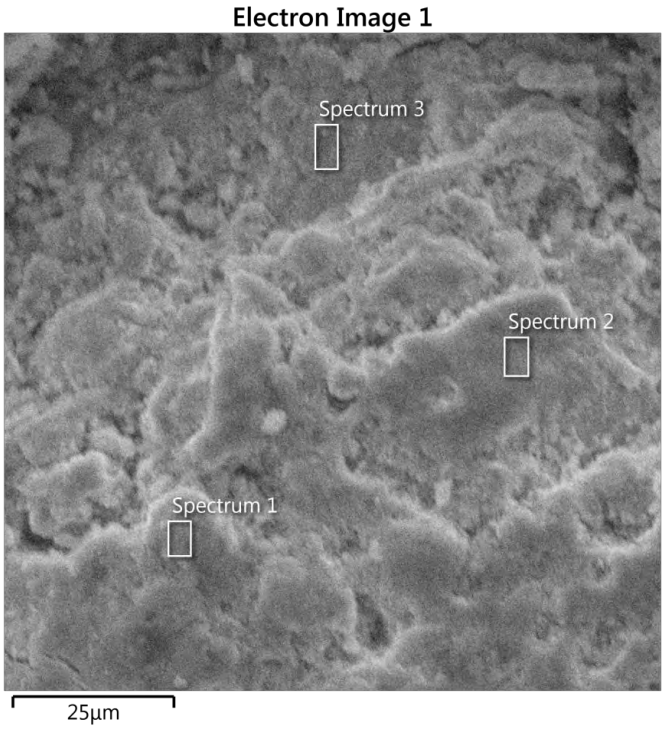

Figure D 1: Selected spectrums from image for ambient cured specimen of mix F70-G15-S15 under EDS analysis.

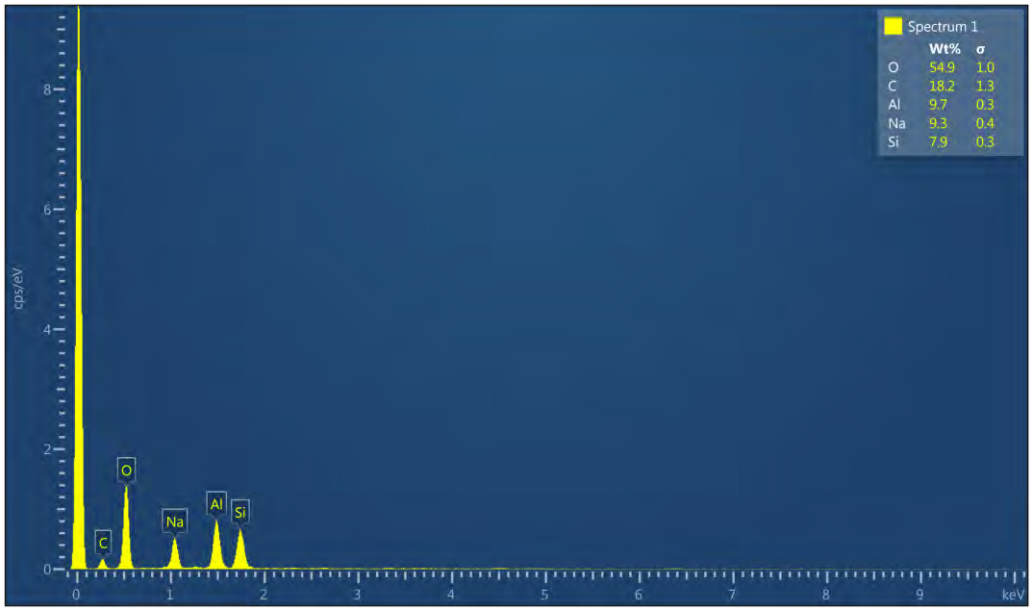

Figure D 2: Chemical composition at spectrum 1 of mix F70-G15-S15.

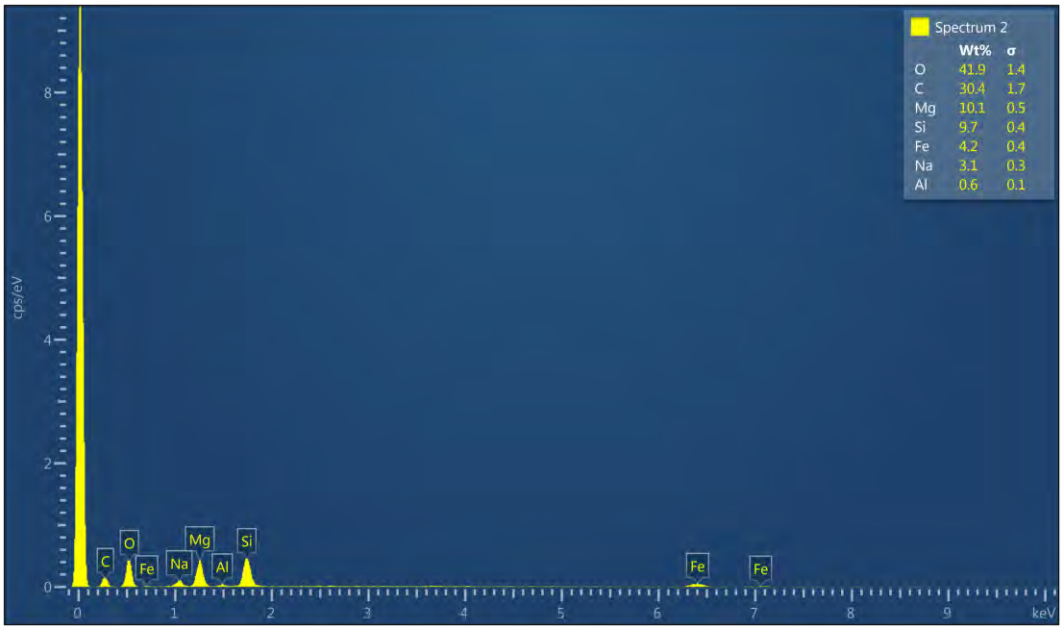

Figure D 3: Chemical composition at spectrum 2 of mix F70-G15-S15.

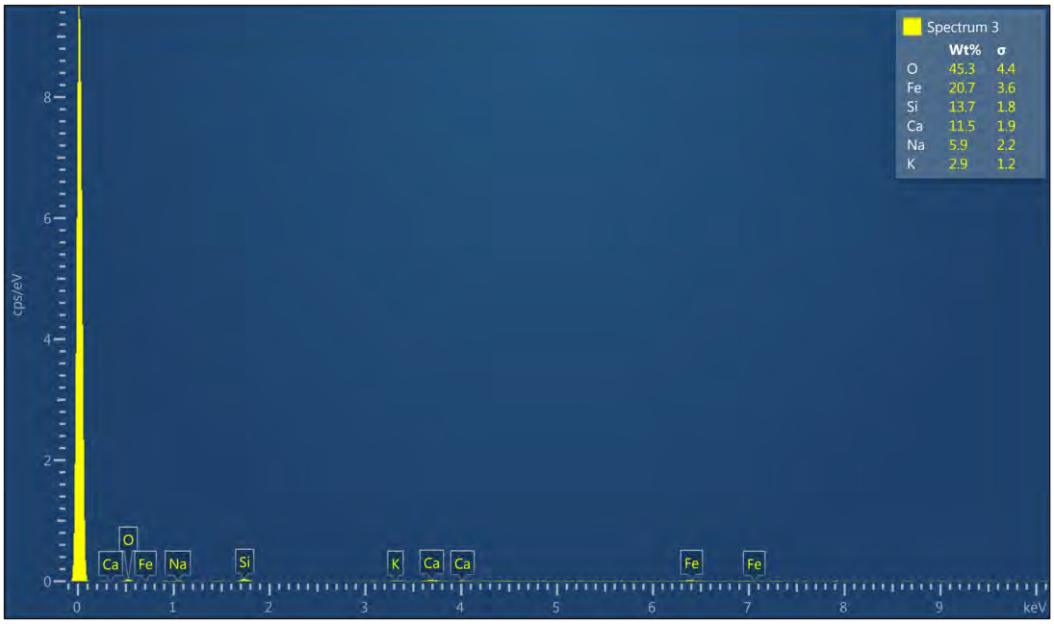

Figure D 4: Chemical composition at spectrum 3 of mix F70-G15-S15.

Appendix E: SEM and EDS for oven cured specimen of mix F70-G15-S15

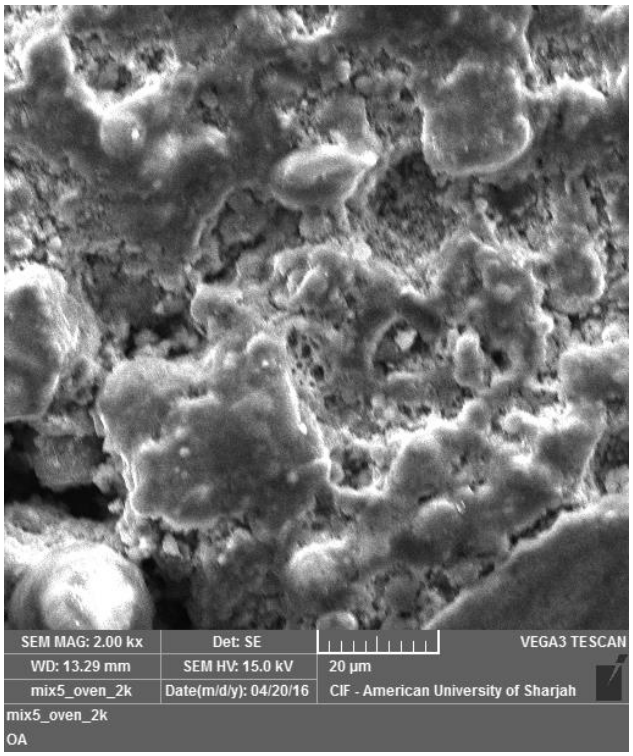

Figure E 1: Oven cured specimen of mix F70-G15-S15 under SEM.

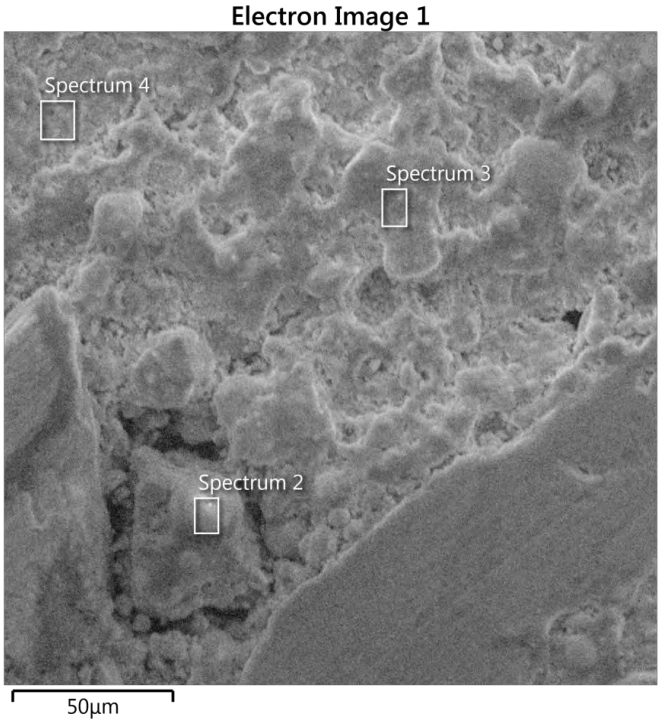

Figure E 2: Selected spectrums from image for oven cured specimen of mix F70-G15-S15 under EDS analysis.

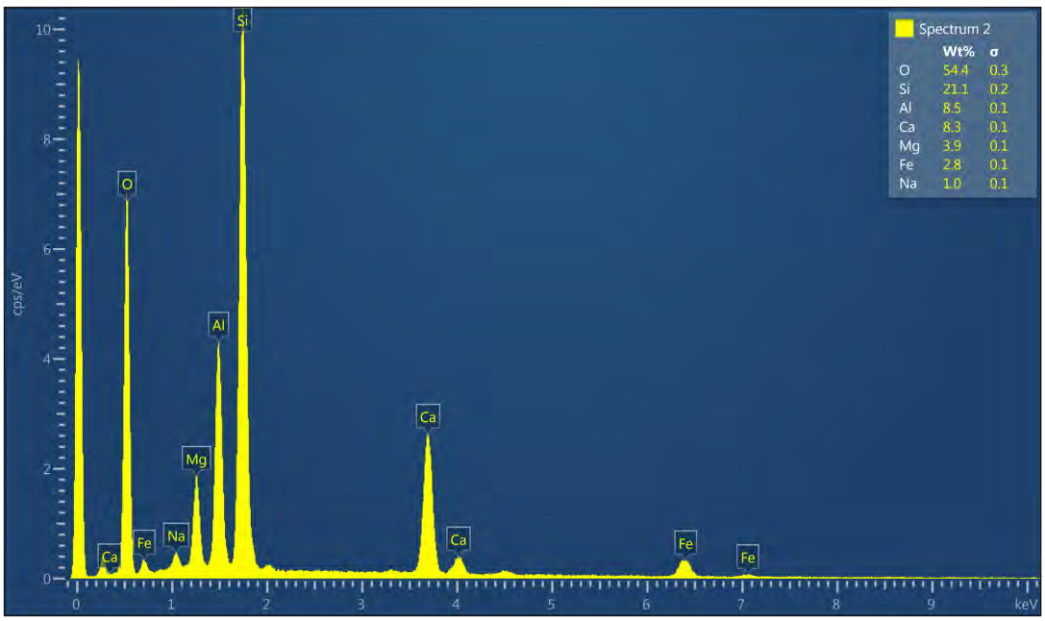

Figure E 3: Chemical composition at spectrum 2 of oven cured specimen of mix F70-G15-S15.

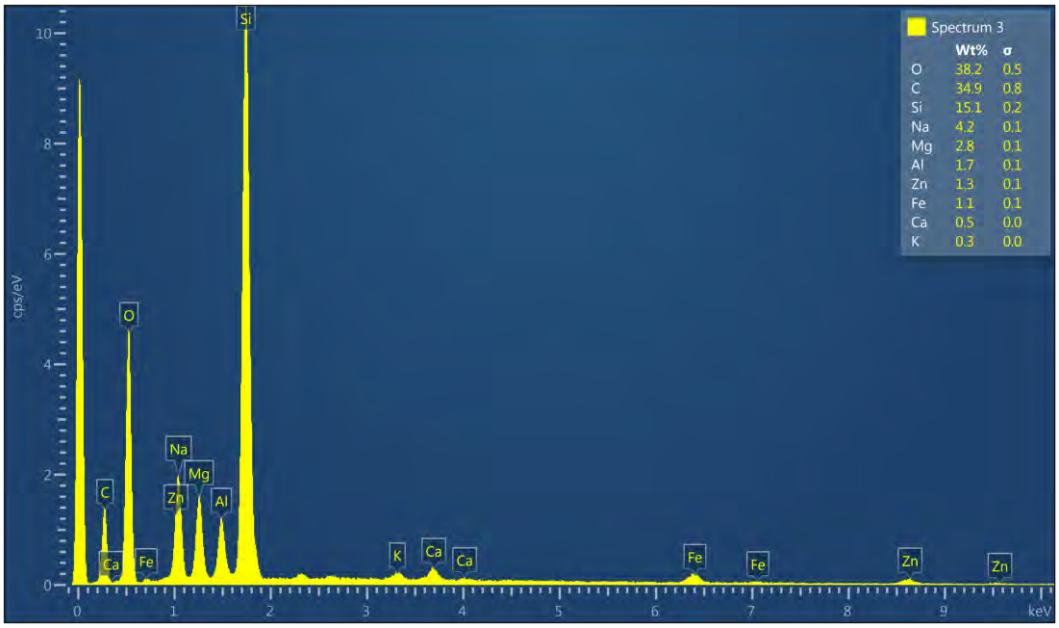

Figure E 4: Chemical composition at spectrum 3 of oven cured specimen of mix F70-G15-S15.

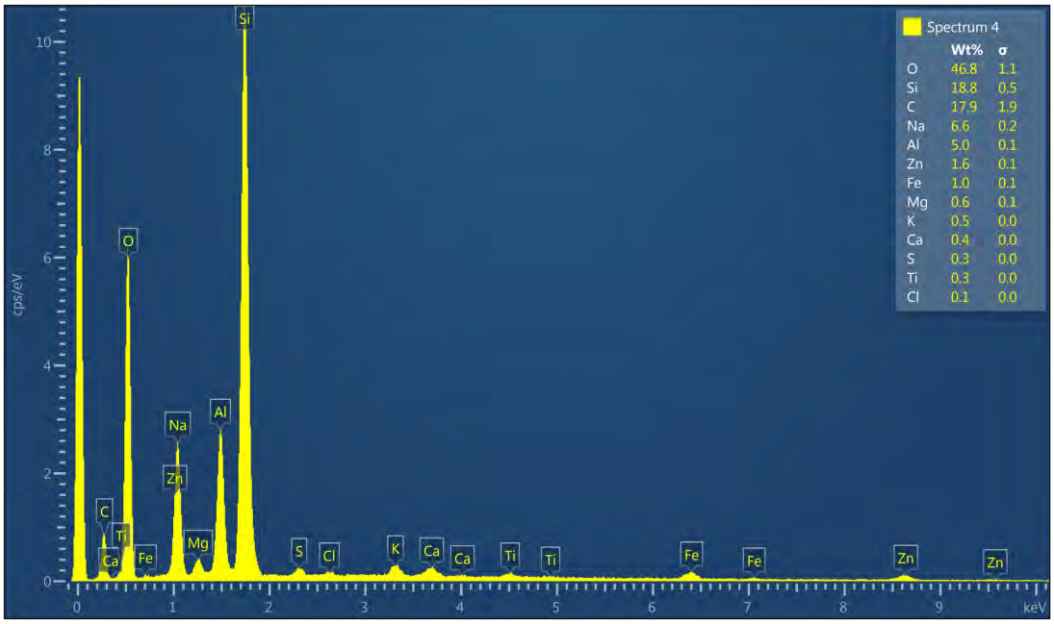

Figure E 5: Chemical composition at spectrum 4 of oven cured specimen of mix F70-G15-S15.

Appendix F: EDS for ambient cured specimen of mix F85-S15

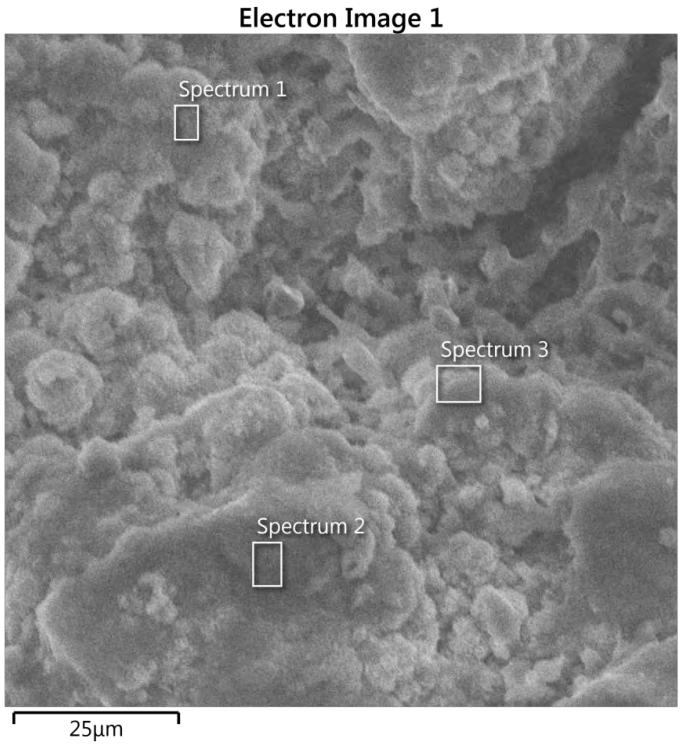

Figure F 1: Selected spectrums from image for ambient cured specimen of mix F85-S15 under EDS analysis.

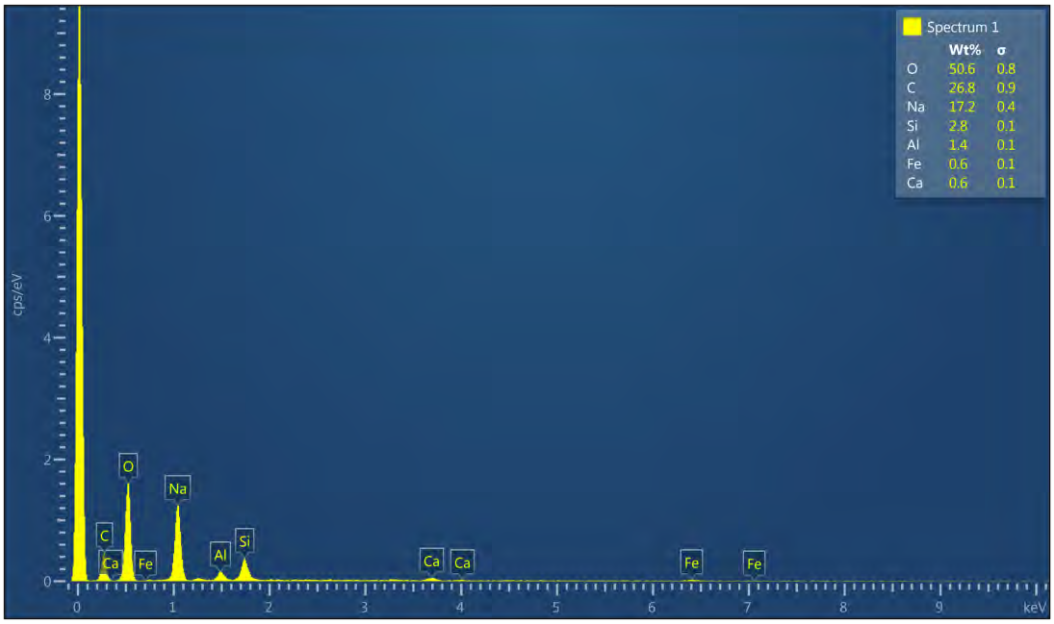

Figure F 2: Chemical composition at spectrum 1 of ambient cured specimen of mix F85-S15.

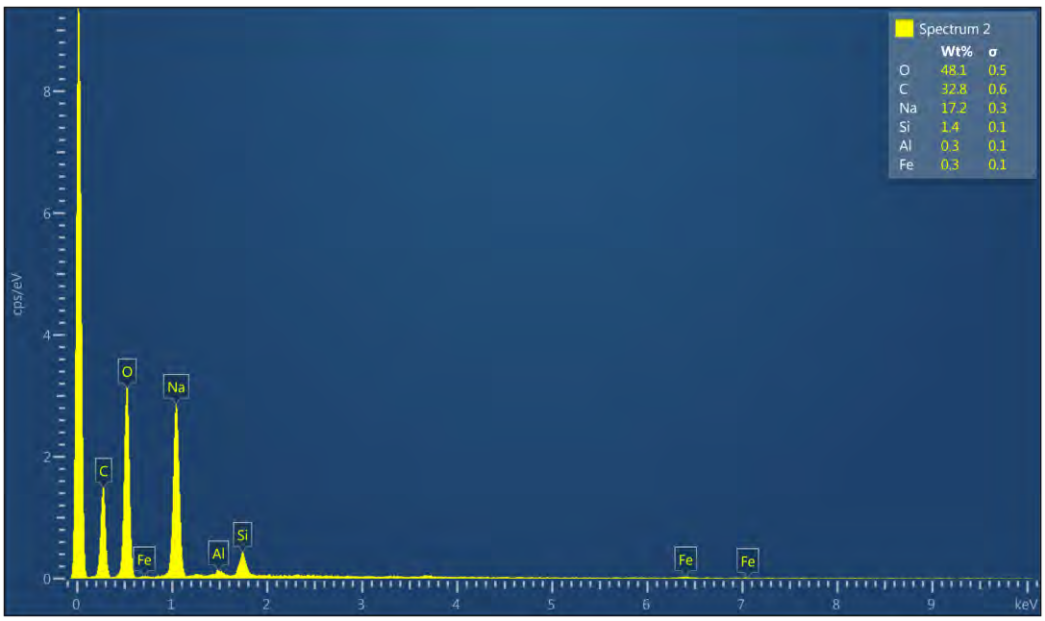

Figure F 3: Chemical composition at spectrum 2 of ambient cured specimen of mix F85-S15.

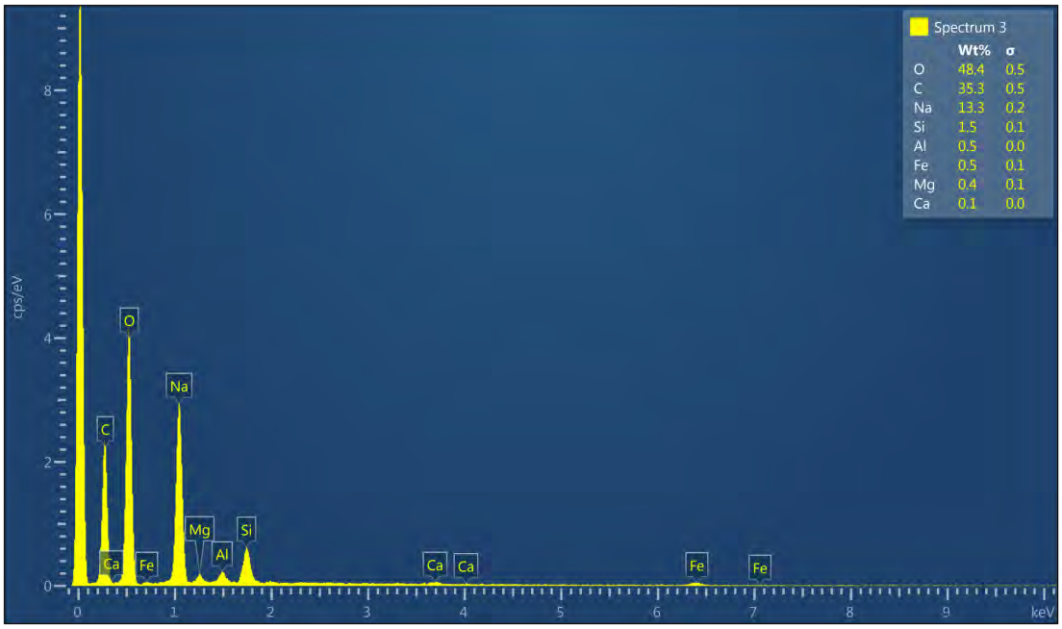

Figure F 4: Chemical composition at spectrum 3 of ambient cured specimen of mix F85-S15.

Appendix G: SEM and EDS for oven cured specimen of mix F85-S15

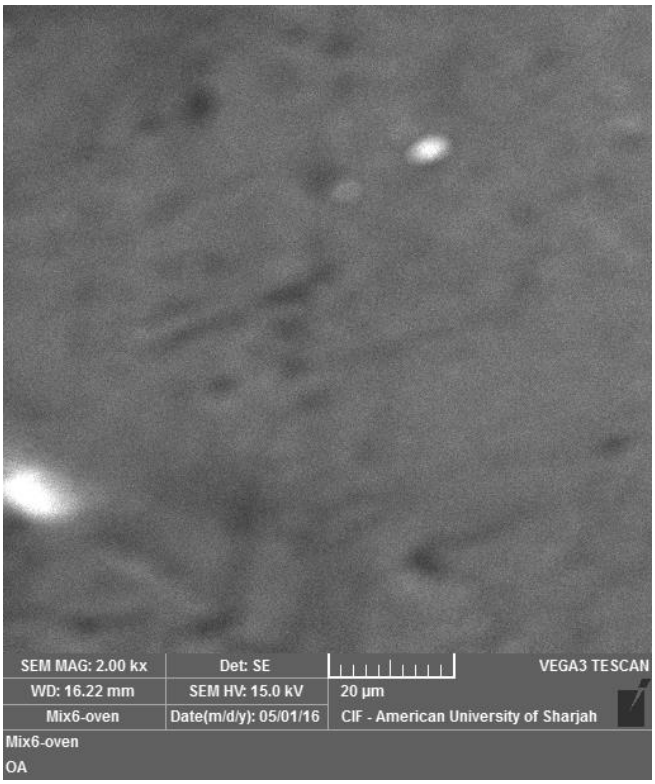

Figure G 1: Oven cured specimen of mix F85-G15 under SEM.

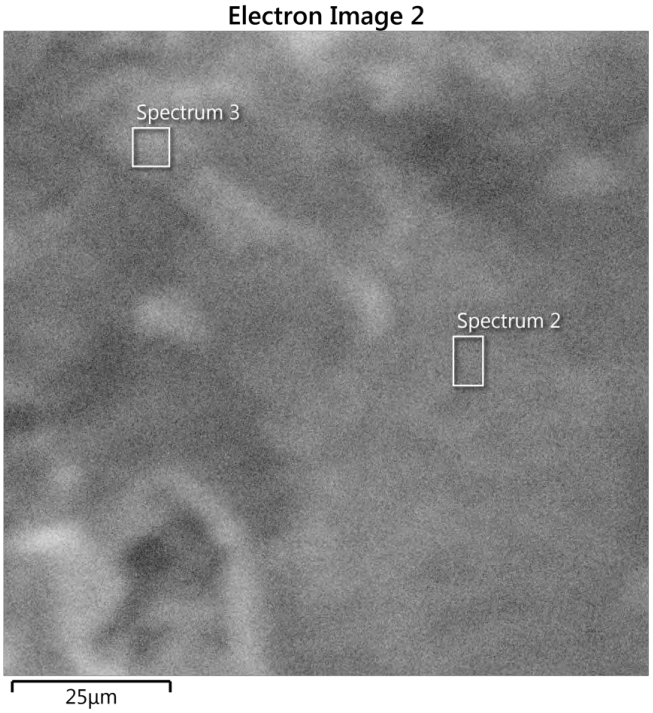

Figure G 2: Selected spectrums from image for oven cured specimen of mix F85-S15 under EDS analysis.

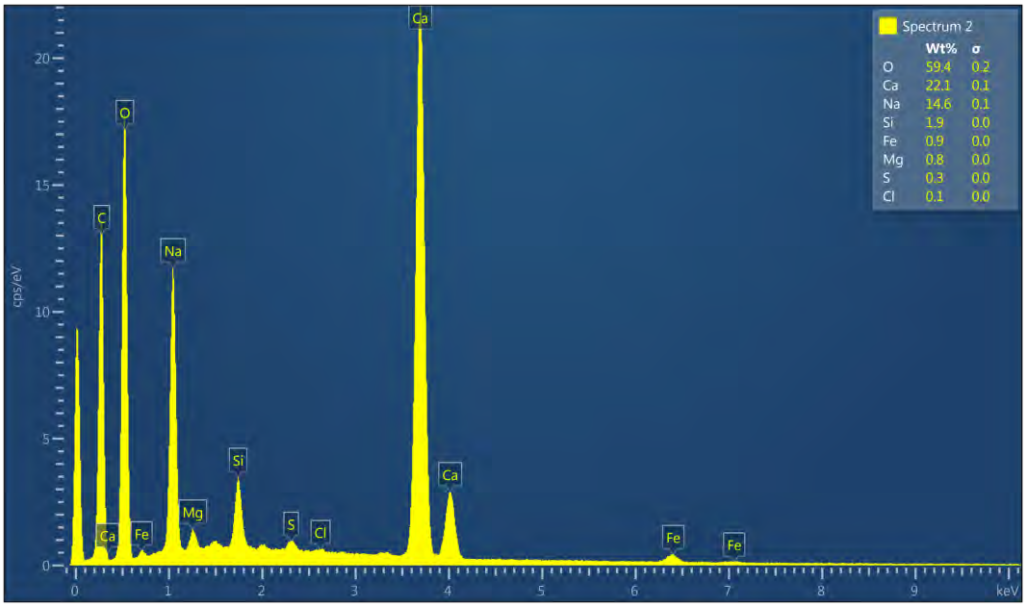

Figure G 3: Chemical composition at spectrum 2 of oven cured specimen of mix F85-S15.

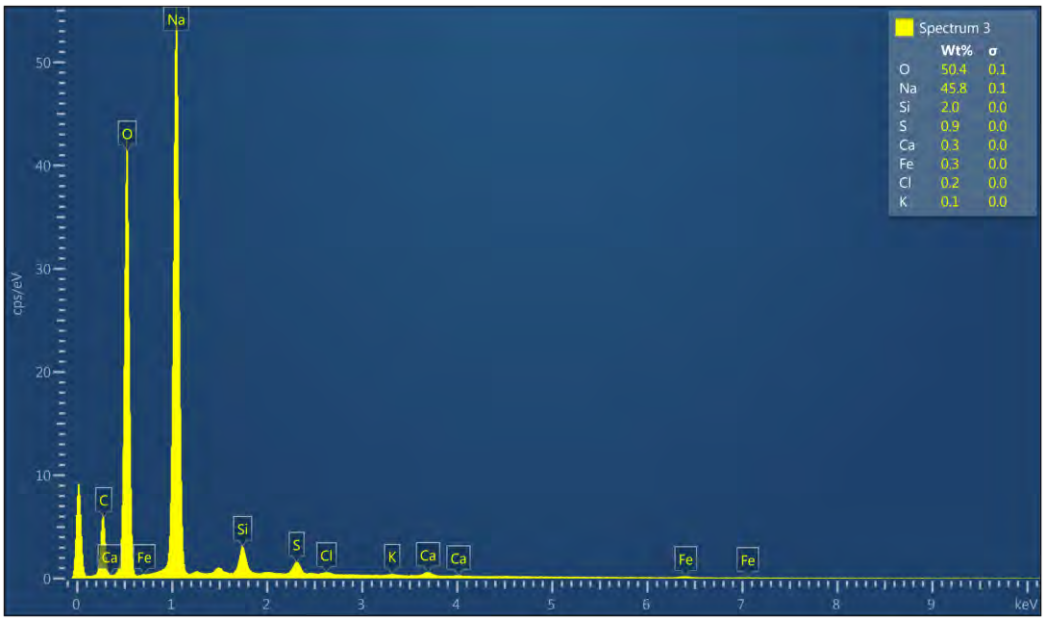

Figure G 4: Chemical composition at spectrum 3 of oven cured specimen of mix F85-S15.

Vita

Ghina M. Zannerni was born in November, 1989, in Dubai, United Arab Emirates. She was educated in local public schools in Sharjah and graduated in 2008. She studied civil engineering at the American University of Sharjah and graduated with a Bachelor of Science degree in January, 2014.

In February 2014, Ms. Zannerni began a Master‘s program in Civil Engineering at the American University of Sharjah. She received a graduate teaching assistantship and worked as a laboratory teaching assistant throughout her graduate study.

Since that time, Ms. Zannerni has published a paper in international conference regarding the effect of cementitious materials on light weight aggregate concrete.